

A synthesis of feasible control methods for floating wind turbines

Kamran Ali Shah^{a,b,c,*}, Ye Li^{a,b,c}, Ryozo Nagamune^d, Dr. Fantai Meng^{a,b,c}, Yarong Zhou^{a,b,c}

^a*School of Naval Architecture, Ocean & Civil Engineering, Shanghai Jiao Tong University, Shanghai 200240, China*

^b*Multi-function Towing Tank, Shanghai Jiao Tong University, Shanghai 200240, China*

^c*State Key Laboratory of Ocean Engineering, School of Naval Architecture, Ocean & Civil Engineering, Shanghai Jiao Tong University, Shanghai 200240, China*

^d*Department of Mechanical Engineering, The University of British Columbia, Vancouver, BC, Canada V6T1Z4*

Abstract

Wind energy has become a viable renewable energy source, and it has abundant potential in both onshore and offshore regions. The wind turbine is encouraged to implement in the deep waters with the support of floating platforms for better wind profile and larger potential than onshore wind. However, the wave load acting on the platform, coupled with varying wind load, introduces a dominant disturbance to its stability. During the operation, the motion uncertainty of the platform tends to compromise the system's performance in terms of power maximization, power regulation, and load mitigation. Various controllers are reported in the literature to deal with the platform instability of floating wind turbines. However, it is a great challenge to achieve optimal power, power regulation, and acceptable load mitigation in the presence of incident wind and waves. This paper presents a review of the published control algorithms used to suppress the platform's motion and evaluates their performance with respect to platform motion minimization, load mitigation, power optimization, and regulation. Potential controller performance improvement based on predicted incident wind and wave is discussed. Recommendations and suggestions for further research are also provided at the end.

Keywords: Floating Offshore Wind Turbines, Floating Platforms, Wind turbine control, Wind energy

*Corresponding author
Email address: ye.li@sjtu.edu.cn (Ye Li)

1 **Nomenclature**

2	ANFIS	Adaptive Neuro-Fuzzy Inference System
3	ANN	Artificial Neural Network
4	AR	Auto-Regressive
5	ARIMA	Auto-Regressive Integral Moving Average
6	ARMA	Auto-Regressive Moving Average
7	BEM	Blade Element Momentum
8	CBP	Collective Blade Pitch
9	CBPC	Collective Blade Pitch Control
10	DOF	Degree of freedom
11	DAC	Disturbance Accommodating Control
12	DMD	Dynamic Mode Decomposition
13	EMD	Ensemble Mode Decomposition
14	ESPRIT	Estimation of Signal Parameters via Rotational Invariance Techniques
15	ELM	Extreme Learning Machine
16	FAST	Fatigue Aerodynamics Structures and Turbulence
17	FOWT	Floating Offshore Wind Turbine
18	GSPI	Gain-Scheduled Proportional-Integral
19	GP	Gaussian Process
20	HAR	Hammerstein Auto-Regressive
21	HAWC2	Horizontal Axis Wind Turbine Code-Second generation
22	HAWT	Horizontal Axis Wind Turbine

23	HMD	Hybrid Mass Damper
24	IBP	Individual Blade Pitch
25	IBPC	Individual Blade Pitch Control
26	IEA	International Energy Agency
27	LSSVM	Least Square Vector Support Machine
28	LCOE	Levelized Cost of Energy
29	LIDAR	Light detection and ranging
30	LPV	Linear Parameter Varying
31	LQR	Linear Quadratic Regulator
32	MLC	Machine learning control
33	MPC	Model Predictive Control
34	MBS	Multi-Body System
35	MIMO	Multi-Input Multi-Output
36	NREL	National Renewable Energy Lab
37	P_{rated}	Rated Power
38	PI	Proportional Integral
39	V_{rated}	Rated Wind Speed
40	RNN	Recurrent Neural Network
41	SISO	Single-Input Single-Output
42	SINDy	Sparse Identification of Nonlinear Dynamics
43	SMC	Sliding Mode Control
44	SC	Structural Control

45	SVM	Support Vector Machine
46	TRL	Technology Readiness Level
47	TLP	Tension leg platform
48	TMD	Tune Mass Damper
49	TLD	Tuned Liquid Damper
50	V_{cut-in}	Cut-in wind speed
51	$V_{cut-off}$	Cut-off wind speed
52	V_{rated}	Rated wind speed
53	V_{wind}	Wind speed

54 **1. Introduction**

55 Wind energy is one of the leading commercial renewable energy resources, and it has significant
56 potential in both onshore and offshore areas [1, 2]. There is a rapid increase in global wind power
57 (onshore and offshore) production in the last decade to utilize this potential, as shown in Figure 1.
58 The total installed capacity for onshore wind turbines has increased from 159GW to 651GW in the
59 last decade. Moreover, an increase in the annual installed offshore wind energy capacity is reported,
60 with a record capacity addition of 6.1GW annual offshore wind energy in 2019. An estimate of new
61 annual offshore installed capacity may exceed 30 GW in 2030, with a compound annual growth rate
62 of 18.6% for the first half and 8.2% during the latter part of the decade, as shown in Figure 2.

63 *1.1. Outlook of Offshore wind*

64 Wind characteristics in the deep sea are more steady, streamlined, and it has a higher annual
65 mean speed than onshore wind [3, 4]. Superior wind quality improves wind energy generation of wind
66 turbines operating in the deep sea. 80% offshore wind energy potential of Europe lies in a water field
67 deeper than 60 meters [5], and therefore, arises a need to install the wind turbine in the deep sea.
68 Additionally, it is encouraged to utilize the offshore wind potential to ease the transition towards
69 renewable energy resources and keep the global temperature at 1.5 degrees Celsius, according to

70 the Intergovernmental Panel’s recommendation on Climate Change (IPCC) [6]. The onshore wind
 71 farms pose environmental harm to human beings and wildlife (i.e., visual and noise impacts) [7–9].
 72 The hazards caused by the land-based wind farms and the low characteristics of onshore wind may
 73 be avoided by installing the wind turbines in the deep offshore regions

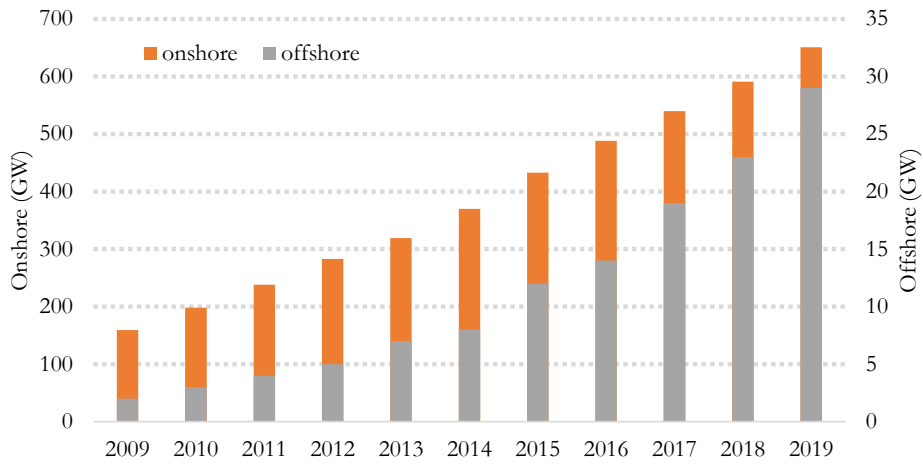


Figure 1: Cumulative installed (onshore and offshore) wind energy capacity of the world (data obtained from [10])

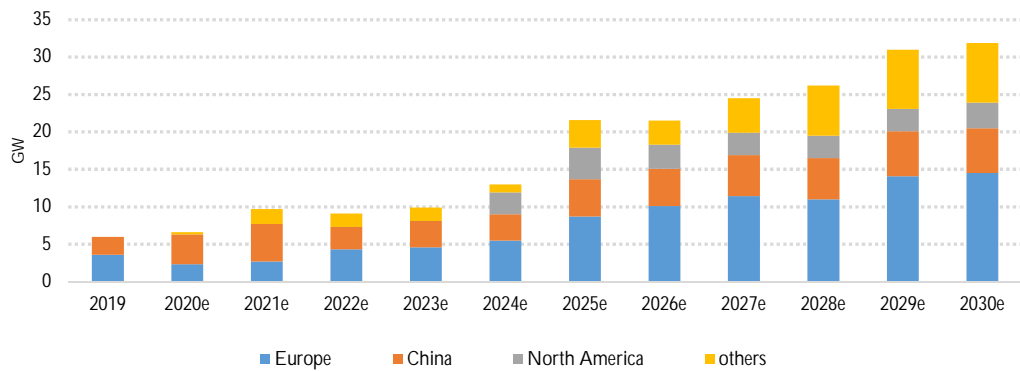


Figure 2: New annual installation prediction until 2030 (data obtained from [11])

74 *1.2. Floating platform and associated problems*

75 Wind turbine placed on top of a floating platform is a feasible solution to operate in deep-sea
76 as the economic constraint hinders the development of a fixed bottom support structure for wind
77 turbines operating beyond 60m water depth. Building a fixed bottom platform for a wind turbine
78 in the deep sea would likely increase the overall cost. Offshore oil and gas exploration in the deep
79 sea greatly relies on floating platforms [12]. Similarly, wind turbines may be operated in the deep
80 ocean using a floating platform attached to the sea bottom. Several concepts exist in the literature
81 to achieve platform stability for FOWT such as Barge, Tension leg platform (TLP), Spar-buoy and
82 Semi-submersible, as shown in Figure 3. These concepts include buoyancy stabilized platforms,
83 mooring lines stabilized platforms, and ballast stabilized platforms . Buoyancy stabilized platforms
84 use submerged body volume to achieve stability, e.g., Barge and Semi-submersible platforms. The
85 tension leg platform (TLP) is a typical example of mooring lines stabilized platform, where the
86 platform is stabilized using mooring lines. In comparison, the spar-buoy is an example of ballast
87 stabilized platform that benefits from the heavy ballasting of the platform's bottom to stabilize
88 the structure. There are two type of wind turbines that are used to generate wind energy i.e.,
89 Horizontal axis wind turbines (HAWTs) and Vertical axis wind turbines (VAWTs), however the
90 scope of this paper is limited to the HAWTs operating in deep-sea.

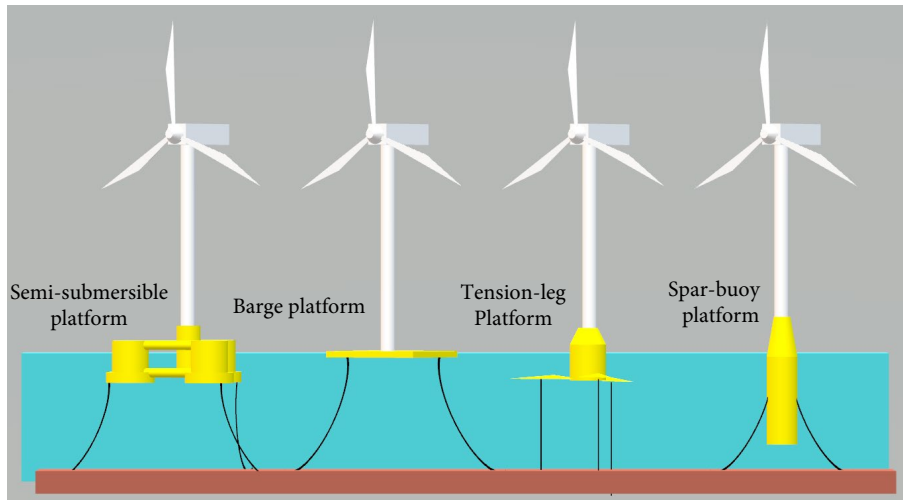


Figure 3: FOWT platforms (Semi-submersible platform, Barge, Tension-leg, and Spar-buoy)

91 Using these floating platforms, wind turbine extract energy from the superior offshore wind

92 operating in the deep ocean. However, floating platforms introduce additional loadings (hydro-
93 dynamic loading, mooring loading) due to incident wave along with the aerodynamic loading on
94 wind turbine. Incident wave associated loadings of floating offshore wind turbine (FOWT) leads
95 to additional 6 degree-of-freedom (DOF) motion compared to the fixed bottom WTs, as shown in
96 Figure 4 where a FOWT is stabilized using a TLP base. The stability of the floating platform is
97 one of the dominant concerns of FOWT technology which may directly impact the performance
98 and safety of FOWTs, leading to increased cost [13].

99 The performance of a FOWT system can be significantly compromised due to the motion of a
100 floating platform. An unstable platform may decrease the nominal wind turbine area and affect
101 energy generation. Platform motions may also increase tower loads compared to fixed bottom
102 wind turbines and negatively impact the system's structural life. Furthermore, it also increases
103 the cost and weakens the economic advantage as compared to onshore wind turbines. Various
104 control algorithms attempt to achieve efficiency and platform motion suppressions by controlling the
105 blade pitch actuator and generator torque of wind turbine. There have been numerous controllers
106 designed to address the shortcomings of floating platform using a range of controllers, such as
107 Proportional Integral (PI), Linear Quadratic Regulator (LQR), Linear Parameter Varying (LPV),
108 and Model Predictive Control (MPC) [14–29]. Some advanced control algorithms utilize the blade
109 pitch mechanism by actuating blades identically (Collective blade pitch) or separately (Individual
110 blade pitch) to provide the wind turbine required aerodynamic thrust to suppress platform motions,
111 maximize power generation and load mitigation. In comparison, Tuned Mass Damper (TMD)
112 based structural control systems [30–33] introduce an extra degree of freedom and decouple the
113 pitching mechanism from providing the required thrust to reduce the pitching phenomena. Advance
114 controllers like MPC based on Light Detection and Ranging (LIDAR) information [25] incorporate
115 the incident wind disturbance before reaching the wind turbine, thus enhancing the performance
116 compared to traditional feedback controllers that function after experiencing incident disturbance.
117 However, the levelized cost of energy cost of energy (LCOE) of FOWT is still higher than the fixed
118 bottom wind turbines. Improved control mechanism may elevate the performance of a FOWT that
119 would lead to reduction in LCOE.

120 The performance of advanced controllers can be improved by incorporating wind and wave fore-
121 cast techniques. Predicted wind and wave information ahead of its encounter with the wind turbine
122 can provide preview based advanced controllers enough time to respond to incoming disturbances

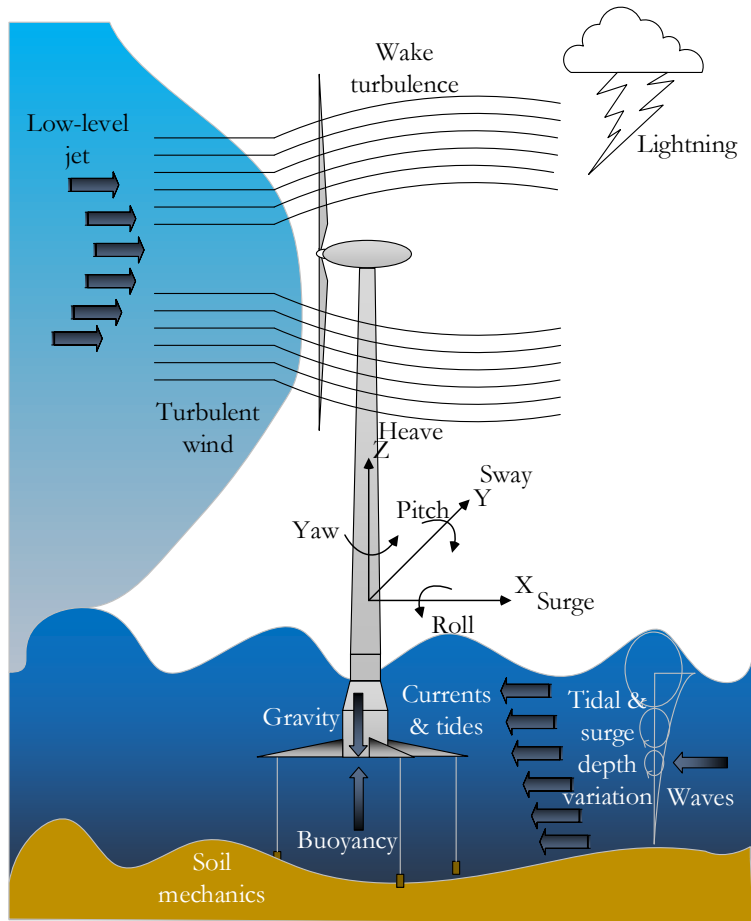


Figure 4: Floating offshore wind turbine in its surroundings

123 and orient wind turbine for optimal and efficient performance. The wind turbine industry is al-
 124 ready benefiting from the wind forecast for wind farm planning, operation, and grid integration
 125 [34]. Numerous forecasting techniques for wind and wave are present in the literature, ranging from
 126 long-term (3 days - 1 week or more) to short-term (few seconds – 30 minutes) prediction horizons
 127 [35–50]. However, the controller response time for FOWT falls in the short-term prediction horizon
 128 category [51, 52]. An accurate short-term disturbance prediction incorporated in modern control
 129 systems, e.g., feed-forward control or MPC, can enhance the performance in terms of platform
 130 stability and loadings and deal with the incident disturbance better than the counterpart feedback

131 controllers, resulting in further lowering the LCOE.

132 1.3. Objective

133 This paper reviews the controllers designed for FOTWs aiming at the platform stability enhance-
134 ment, maximum power generation and structural life extension. A detailed discussion is presented,
135 and potential improvements based on the reviewed controllers are provided. The paper outline is
136 as followed: Section 2 presents the system overview. Control structure and methodologies used
137 for FOWTs are discussed in Section 3. In Section 4, the wind and wave prediction for the control
138 design is introduced. The discussion and the summary is presented in Section 5 and Section 6,
139 respectively.

140 2. System description

141 FOWT operates in the deep sea with an extension of a floating platform attached to the sea
142 bottom with mooring lines. However, the foundation of a FOWT exhibits 6 degrees of motion
143 due to incident wave, as shown in Figure 4. The performance and operation of the wind turbine
144 is coupled with the platform motion. Therefore, it is essential to minimize the platform motions
145 during the operation of FOWT. A description of the operation of the FOWT is provided below.

146 2.1. Wind turbine

147 Wind turbines deployed in the deep sea operate similarly to land-based wind turbines to extract
148 kinetic energy from the wind. Air passes through the blades and causes the rotor to rotate. The
149 rotor is connected to a generator which produces energy. The maximum possible energy extracted
150 from wind is 59.3%, known as the Betz limit [53]. Maximum power (P_{max}) generated by a wind
151 turbine in a given scenario can be calculated by the following formula, as shown in Figure 5.

$$152 \quad P_{\max} = \frac{1}{2} \rho A v^3 C_p(\lambda, \beta) \quad (1)$$

$$\lambda = \frac{\Omega R}{v} \quad (2)$$

153 where

- 154 • ρ = Air density

- 155 • A = Swept Area
- 156 • C_p = Power coefficient (based on tip-speed ratio (λ) and blade pitch angle β)
- 157 • R = Rotor radius
- 158 • Ω = Angular speed
- 159 • v = Wind speed

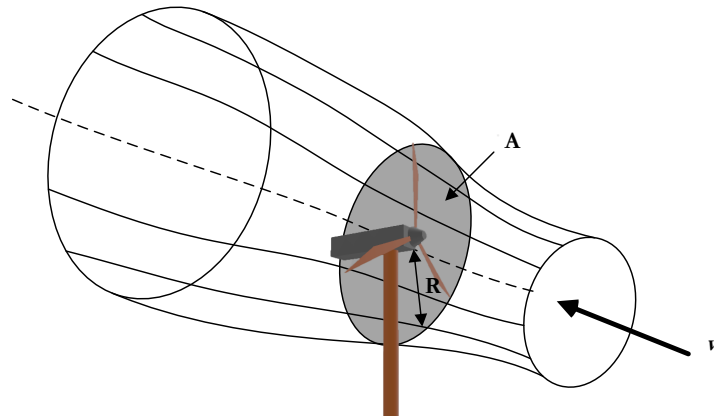


Figure 5: Wind energy extraction using wind turbine

160 The incoming wind speed is an essential factor in the control system design, control objectives
 161 and operation of wind turbines. The operating spectrum of a wind turbine is divided into three
 162 significant regions, as shown in Figure 6. In region I, the wind speed is less than the cut-in wind
 163 speed ($V_{\text{cut-in}}$), and the wind turbine is in parked condition. In region II, the wind speed value is
 164 less than the rated value (V_{Rated}). The control objective focuses on the maximum energy extraction
 165 from the wind by keeping the blade pitch at an optimal angle. In region III, where the wind speed
 166 value surpasses the (V_{Rated}), the objective shifts towards regulating generated power with pitch
 167 angle activity. When the wind speed reaches cut-off wind speed ($V_{\text{cut-off}}$) the mechanical brakes are
 168 applied for the safety of wind turbine. In the case of FOWTs, the number of control objectives are
 169 increased with the consideration of platform motion. For a FOWT, the floating platform, regardless
 170 of being tied to the seabed, may generate significant problems due to incident waves and wind loads.

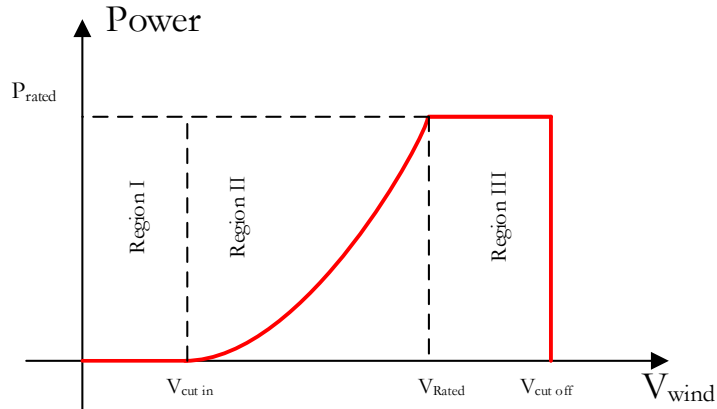


Figure 6: Operating regions of a wind turbine

171 *2.2. Framework of FOWT control systems*

172 FOWTs are prone to platform motions due to floating base which leads to performance deteriora-
 173 tion. However, an effective control system may deal with the platform motions and achieve optimal
 174 wind energy generation. Existing control mechanisms for fixed bottom wind turbine are rendered
 175 infeasible for FOWTs due to the additional platform motion of FOWT. However, fixed-bottom
 176 wind turbine controllers may be modified to include the platform motion suppression objective.

177 Majority of the FOWT controllers are based on feedback control mechanism. In addition, there
 178 are advanced feed-forward controllers available in the literature as well. A detail discussion on
 179 these controllers is given in the Section 3. The benefit of feedforward mechanism may be further
 180 extrapolated by using incident wind and wave forecast to improve the controller performance. An
 181 account of incident wind and wave forecast is given in Section 4.

182 **3. FOWT Control structure**

183 Control system of a wind turbine is responsible for handling the aerodynamic wind load and
 184 converts the wind energy into electric power. In general, there are multiple control levels to deal
 185 with the wind turbine operation. The primary-level supervisory control level deals with the startup
 186 and shutdown of the wind turbine. The wind turbine is only started up when there is enough
 187 wind, and shutdown is triggered in the presence of excessive wind, as it may harm the wind turbine
 188 structure. The second-level operational control is dedicated to achieving control objectives based

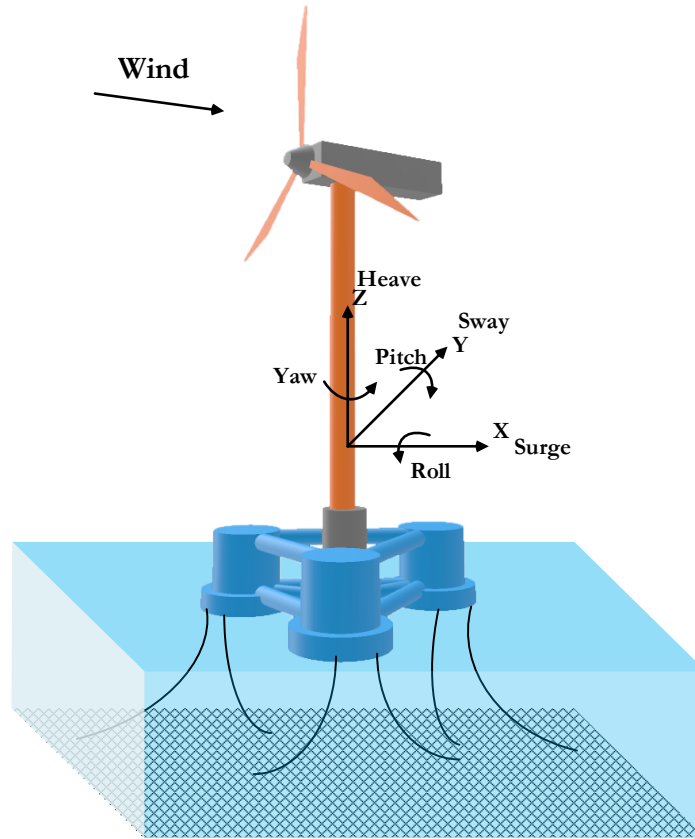


Figure 7: Associated platform motions of FOWT

189 on the wind turbine operating region, as shown in Figure 6. In comparison, the third-level control
 190 is concerned with the yaw and pitch actuation system and related electronic units. The scope of
 191 this paper is limited to the second-level operational control of a wind turbine. Later in this section,
 192 the control objectives and control methodologies used to achieve these objectives for FOWTs are
 193 discussed in detail.

194 *3.1. Control objectives*

195 Control objectives of a wind turbine vary based on the operating regions, namely maximum
 196 power generation operating in region II and power regulation in III, as shown in Figure 6. There
 197 are generally two control loops to achieve these control objectives, as shown in Figure 8. Operating
 198 in region II, the torque control loop of the wind turbine is used to maximize the generated power
 199 by operating near the optimal C_p by using fixed blade-pitch angle to an optimal value, based
 200 on equation 3. In region III, the objective shifts towards regulating the generated power at the
 201 rated value. The blade-pitch control loop regulates the aerodynamic loads and generated power
 202 by manipulating the blade pitch value. There are two standard pitching strategies for the region
 203 III pitch control loop, pitch-to-stall and pitch-to-feather [54]. The generator torque control while
 204 operating in region III, is calculated based on the relationship in equation 3.

205 However, the major problem associated with FOWT occurs due to platform motion while op-
 206 erating in region III. The wind turbine structure undergoes undesired pitching phenomena, often
 207 called negative pitching [55]. The frequency of the platform is coupled with the blade pitch mecha-
 208 nism while operating in region III, causing a surge in the pitching motions of the platform leading
 209 to issues like poor power quality and increased loads. Therefore, an adequate control mechanism to
 210 achieve the standard wind turbine control objectives and deal with the platform pitching phenomena
 211 associated with floating platform of FOWT is needed.

$$T_{gen} = \frac{\pi \rho R_{rotor}^5 C_{p,max}}{2\lambda_o^2 N^3} \omega_{gen}^2 = K \omega_{gen}^2 \quad (3)$$

$$T_{gen} = \frac{P_{rated}}{\eta_{gen} \omega_{gen}} \quad (4)$$

212 where

- 213 • T_{gen} =Generator torque
- 214 • ρ = Air density
- 215 • R_{rotor} = Rotor radius
- 216 • N = Gear box ratio
- 217 • $C_{p,max}$ = Maximum power coefficient

- 218 • λ_o = tip speed ratio related to $C_{p,\max}$
- 219 • ω_{gen} = Generator rotational speed
- 220 • η_{gen} = Generator efficiency
- 221 • P_{rated} = Rated generated power

222 A range of system models are available in the literature, that are used to develop control schemes
 223 for FOWT and preview the outcome without running the actual wind turbines. Appendix A
 224 contains the details of these simulation codes for the readers further interested in FOWT system
 225 models.

226 3.2. Control methodologies

227 Control methodologies for FOWT to deal with the undesired platform associated motions while
 228 operating the wind turbine at optimal level are based on traditional single-input single-output
 229 (SISO) and advanced multi-variable multiple-input-multiple-output (MIMO) mechanisms. This
 230 section provides a discussion on the range of these controllers reported in the literature.

231 3.2.1. Traditional FOWT controllers

232 The traditional FOWT controllers are simple and easy to design control mechanisms that are
 233 based on the single-input single-output (SISO) principle. Independent control loops are applied in
 234 parallel to achieve multiple control objectives, as shown in Figure 8.

235 Platform pitching motion of FOWT was minimized by keeping the frequency of the blade pitch
 236 mechanism lower than the resonance frequency of the platform by Larsen et. al [14]. For region
 237 2, a variable speed control loop was used to maximize the generated power. A region of constant
 238 speed was introduced between regions 2 and 3, followed by a constant torque loop in region 3.
 239 Pitching action is determined by a gain-scheduled proportional-integral (GSPI) controller for region
 240 3. Improved platform pitching was achieved using less aggressive control methodology at the cost
 241 of lowered power quality and poor rotor speed regulation.

242 Another GSPI controller based solution for negative platform damping problem of barge based
 243 FOWT was provided by Jonkman [15]. Two independent SISO controls were designed; A generator-
 244 torque controller to generate maximum power in region 2 and keep the power captured at the rated
 245 value in region 3. A GSPI controller was considered to adjust rotor speed as a function of blade pitch

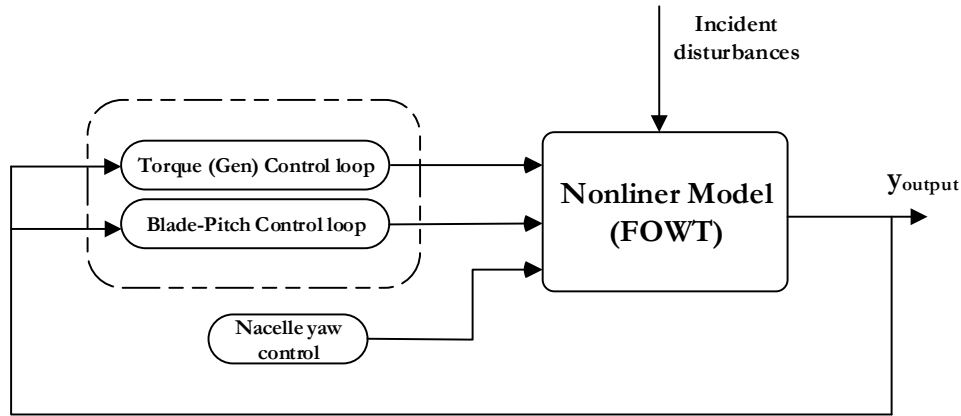


Figure 8: Wind turbine standard control loops

246 activity based on the collective blade pitch (CBP). Jonkman et al. [15] designed additional control
 247 loops upon facing complications regarding platform oscillations and power fluctuation during the
 248 early design synthesis. Tower-top feedback control, active pitch-to-stall control and a controller
 249 based on detuned gains were the additional loops included in the original design mechanism. These
 250 additional loops were proposed to minimize the fore-aft motion of the tower, instability of platform
 251 yaw, and excessive barge motions, respectively. Tower top feedback control failed to improve the
 252 pitching motions of the platform.

253 Furthermore, active pitch-to-stall control was found good at power regulation for the barge
 254 platform at the expense of increased platform pitching motion. Whereas, detuned gains proved
 255 to be the most suited controller among others, as it reduced the blade activity and addressed
 256 the platform pitching issue. This configuration is used for testing newly designed controllers and
 257 labeled as baseline FOWT control [56]. The use of individual blade pitch (IBP) and multiple-input-
 258 multiple-output (MIMO) state-space controllers were suggested to enhance performance further.

259 Baseline controller designed by Jonkman et al. [15] was analyzed for different platforms by
 260 Matha et al. [57]. The TLP, Barge, and Spar-buoy floating concepts were compared concerning
 261 fatigue loads and platform stability. Matha et al [57] modified the baseline controller for the spar-
 262 buoy platform. Constant torque control was designed to improve the platform pitching motion while
 263 operating in region 3, contrary to a constant power controller originally designed by Jonkman et al.

264 [15]. Meanwhile, the controller's bandwidth was kept low to avoid coupling with the frequency of
265 the platform. It was noticed that the barge platform is cost-effective, but its inability to withstand
266 incident loads may cause stability issues. The spar-buoy platform showed resistance towards tower
267 loading as compared to the barge platform. However, the deployment of the spar-buoy platform
268 is costly due to its intricate design and assembly. In comparison, TLP was found to have better
269 performance among the compared concepts. However, it was found that the anchoring system of
270 TLP may increase the cost.

271 Platform instability was addressed by using the pitching velocity as an input to regulate the
272 generator rated speed in region 3 [16]. The generator speed was used to provide the counter thrust to
273 suppress the platform pitch motion and achieve platform stability. This unique control methodology
274 reduced negative damping and blade pitch activity at the cost of acceptable rotor speed fluctuations
275 and power variation. In a subset simulation, Individual blade pitch control (IBPC) was implemented
276 using the Coleman transformation [58] to reduce blade loads. However, the IBPC increased the
277 blade pitch activity resulting in inadequate blade load reduction.

278 A control strategy based on the estimation of wind speed to suppress the negative damping for
279 the Hywind concept platform [55] was proposed by Skaare et al. [17]. The control mechanism de-
280 signed by Skaare et al. [17] improved the tower loading and the nacelle oscillations. Simultaneously,
281 the poor rotor speed regulation and the reduced power generated were observed compared to the
282 conventional blade pitch mechanism. Moreover, since the strategy was based on the estimated form
283 of wind in region 3, this control scheme's effectiveness was mainly governed by the wind estimation
284 quality.

285 *3.2.2. Advanced control methods*

286 The classical SISO controllers are easy to realize controllers, however may not be a suitable op-
287 tion for highly coupled multi-objective systems like FOWTs. The design process of SISO controllers
288 requires a thorough understanding of the system and careful tuning of control loops separately. Oth-
289 erwise, multiple control loops may couple with each other and affect the overall system operation.
290 As suggested by Jonkman et al. in [15], advanced controllers based on multi-input multi-output
291 (MIMO) may further improve the performance of FOWT due to its inherent ability to deal with
292 short comings of SISO control. Multi-variable MIMO control schemes such as Linear Quadratic
293 Regulator Control (LQR), Linear Parameter Varying control (LPV), Model Predictive Control

294 (MPC), used for FOTWs reported in the literature are described below.

295 Most of the advanced controller designed for FOWT are based on State-space control. State-
296 space control design involves linearizing the non-linear system model at an operating point x_{op} such
297 that state x transforms into the deviation Δx around the x_{op} . Later, linear control theory is applied
298 to design a controller to achieve the given objectives. State-space equation is shown below,

$$\begin{aligned}\Delta\dot{x} &= A\Delta x + B\Delta u + B_d\Delta u_d \\ \Delta y &= C\Delta x + D\Delta u + D_d\Delta u_d\end{aligned}\tag{5}$$

299 where

- 300 • $x = x_{op} + \Delta x$
- 301 • y = Measurement matrix
- 302 • u = Actuator matrix
- 303 • Δu_d = Disturbance matrix
- 304 • A = State matrix
- 305 • B = Actuator Gain matrix
- 306 • B_d = Disturbance gain matrix
- 307 • C = Output matrix
- 308 • D = Feed-through inputs
- 309 • D_d = feed-through disturbance

310 Several advanced controllers were designed using MIMO state-space methodology on Barge,
311 TLP, and Spar-Buoy platform based FOWT [20–22]. The collective blade pitch controller (CBPC)
312 and IBPC were designed for a barge platform [20]. The IBPC and wind disturbance-based Dis-
313 turbance Accommodating Control (DAC) were designed for FOWTs on a barge, and TLP [22].
314 The controllers designed for Barge and TLP were later used to investigate the performance of the
315 Spar-buoy platform [21]. In region 3, the CBPC scheme for FOWT showed improvements in better
316 speed regulation, mainly due to constant power control instead of constant torque control and the
317 platform pitch motion reduction.

318 IBPC was utilized to deal with the overlapping blade pitch commands issued for the rotor speed
319 control and the platform pitch minimization [21]. IBPC mechanism improved tower loading for the
320 barge platform. In comparison, the performance of IBPC was found limited due to the relatively
321 lower platform frequency spar-buoy platform. On the other hand, DAC has an advantage due to
322 improved rotor and power regulation based on increased blade pitch actuation for the spar-buoy
323 platform.

324 Controller-based on IBP achieved improvements when applied to the Barge platform compared
325 to the CBP control [20]. DAC was rendered not useful for barge platform because the barge platform
326 is mainly influenced by waves; however, DAC is used to influence wind disturbances. [22]. IBPC
327 was shown to have improvements regarding rotor speed and power regulations for Barge and TLP,
328 but for Spar-buoy, when dealing with the platform pitching, this scheme was not as effective due
329 to the low natural frequency of the platform. Further improvements related to power and speed
330 regulations were achieved using DAC for the TLP platform.

331 A study was conducted on the input-output relation of the 10MW FOWT to find out the
332 frequencies with a substantial impact on the output with the least control variable impact by F.
333 Lemmer et al. [23]. The wave information was added to produce a realistic environment and
334 representation of the coupled frequencies with the parametric wave excitation model from [59].
335 Wind and wave disturbances with significant impact on the output due to the minimum control
336 actuation were chosen. This information was used to design an LQR controller based on input blade
337 pitch angle and generator torque, and a comparison to a conventional PI controller was made. The
338 designed controller was noticed to have improvements concerning system response reduction and
339 damping various resonances. However, the control mechanism could not completely overcome the
340 effect of incoming wave disturbance.

341 Gain scheduled output feedback H-infinity control based on collective blade pitch approach for
342 FOWT operating in region 3 was designed by T. Bakka et al. [18]. A simplified model is generated
343 based on significant FAST model dynamics for control synthesis, namely, the rotor generator and
344 tower. Linear models are generated at multiple operating points based on output feedback H-infinity
345 control, and a scheduling mechanism is developed. Substantial improvements were found in terms
346 of the tower loadings and rotor speed regulation.

347 Linear Parameter Varying (LPV) and Linear Quadratic Regulator (LQR) developed by using
348 gain-scheduled (GS) blade pitch controller for a barge platform-based FOWT [19]. The objective

349 was to regulate the generated power and minimize structural loadings while operating in region 3.
350 The LPV was further modified with the state feedback and output feedback control mechanisms
351 and compared with the baseline wind turbine [15, 60]. It was found that the GS-LPV and GS-
352 LQR controllers performed better in terms of power regulation and platform pitch minimization.
353 Whereas, LPV-GS controller with state-feedback has shown superior improvements in platform
354 pitch motion damping than the rest of the controllers.

355 Input/output feedback linearization (IOFL) and Sliding Mode Control (SMC) methods were
356 used to analyze the effects of incident disturbance on platform motions and regulate generator
357 speed and of FOWTs operating in region 3 [24]. A simplified model based on the DOFs of blade
358 pitch and generator speed, and platform pitch was obtained. Later, a simplified non-linear model
359 based on series of linearized simplified models is designed. The switching mechanism between these
360 linear models is obtained based on the LPV model as a blade pitch angle function. Compared
361 with the baseline model, SMC showed improvements regarding generator speed regulation, while
362 the platform pitch motions were on a similar level as for the baseline wind turbine. The reason
363 for speed regulation was, the wind speed was considered for control design. However, the platform
364 motions were observed without adding to the control design. Contrary to SMC, IOFL control
365 causes increased platform pitching motion when compared with the baseline controller. Another
366 important finding was observed that the performance of the developed controller was degraded
367 when implemented on complex models.

368 Model predictive control (MPC) is an advanced control method that predicts future action
369 based on the internal system model's available information fulfilling a set of constraints. Numerous
370 examples are available in the literature regarding the use of MPC for fixed bottom wind turbines.
371 [61–64]. D. Schlipf et al. [25] designed a non-linear-MPC (NMPC) for FOWTs operating in region
372 3 based on the simplified Sander model [65]. The incident wind and the wave preview was used
373 for the controller design based on CBP and generated torque. The control objective was to keep
374 the generated power and rotor speed steady based on an ideal estimation of the wind and the
375 wave preview [61]. The designed controller was later used on the baseline FOWT [15] placed on
376 a spar-buoy platform under an intense wave and wind profiles. The controller showed satisfactory
377 results regarding the generated power and speed regulation error, including the blade load reduction;
378 However, the NMPC controller requires higher computational resources.

379 Following the CBP-based non-linear MPC design for FOWT in [25], S. Raach et al. [26] came

380 up with an extended version of NMPC based on the IBP mechanism. The IBPC-NMPC included
381 the rotor and the blade load reductions alongside the existing benefits of the original CBP-NMPC,
382 platform pitch reduction and rotor speed regulation. After the controller design, its successful
383 implementation on the baseline wind turbine exposed to the turbulent loads was achieved. The
384 rotor's fatigue loads were reduced significantly by using the extended NMPC based on the IBP
385 mechanism.

386 An optimal linear MPC implemented on a 10 MW FOWT by F. Lemmer et al. [27]. A tunable
387 controller was designed to provide early-stage design assistance during the fabrication of FOWT.
388 The linear-MPC based on the MIMO system was designed to operate in region 3 to regulate the
389 power to a constant value and minimize the structural loads. In comparison, maximum power
390 generation was the primary objective for region 2. Linear-MPC showed adequate improvement
391 than a PI controller for the rotor speed and generator power regulation. Moreover, the tower top
392 movement and negative platform pitch were also minimized.

393 *3.2.3. LIDAR based advanced control*

394 Reduction in LCOE of FOWT may be achieved through enhanced structural performance
395 against incident loads . For this purpose, we have discussed several feedback controllers. One
396 major drawback is that these control mechanisms are designed to respond to the incident impact
397 after its interaction with the system structure. For FOWT, wind turbine structure experiences the
398 incoming wind and wave and feedback control system is activated after the interaction of incoming
399 wind and waves with the system. Such interaction may degrade the structural life over a period
400 of time. Thus traditional controllers may not achieve extended structural life and would increase
401 LCOE subsequently.

402 To circumvent the shortcomings of feedback controllers, the researchers may use feedforward
403 control loops to deal with the incident disturbances before contacting the wind turbine. LIDAR is
404 used to measure the incoming wind disturbance. There have been numerous attempts made to use
405 LIDAR for fixed-bottom wind turbines. [66–68], LIDAR is based on Doppler's principle, where a
406 laser beam is spread out which upon reflection is received [69]. The wavelength of the transmitted
407 and received beam is used to estimate the incoming wind speed. Two types of LIDARs are available
408 based on the wind speed calculation methods, i.e., continuous and pulsed wave. The continuous
409 wave LIDAR uses a laser beam focused at the focal point while the pulsed wave LIDAR calculates

410 wind speed at multiple distances [66].

411 Unlike fixed-bottom wind turbines, preview-based LIDAR assisted control for FOWT is still
412 under development. An extended version of feedforward collective blade pitch control, initially used
413 for fixed-bottom wind turbines in [70], was designed for FOWT using H-infinity control synthesis
414 by S.T. Navalkar et al. [28]. Based on the combination feedforward-feedback newly formulated
415 CBPC was found useful at minimizing the loads and generator speed oscillations. D. Schlipf et al.
416 [29] designed a CBP-feedforward controller for FOWTs based on LIDAR data. The feedforward
417 control was designed using a simplified non-linear model for ideal wind preview and used along with
418 the traditional feedback controller designed by Jonkman et al. [56]. Later, the design procedure
419 was followed by using nacelle-based LIDAR information instead of ideal preview wind. With the
420 addition of wind uncertainty, a realistic feedforward controller proved useful compared with the
421 standalone baseline controller to minimize rotor speed and power fluctuation and reduce blade,
422 rotor shaft, and tower loads, respectively.

423 *3.2.4. Structural control*

424 There is another approach reported in the literature to minimize the structure loadings, and
425 external influences called structural control (SC). In this methodology, extra DOFs are introduced
426 to influence the structural behavior of the system. This methodology has been vastly used to
427 minimize the oscillations and vibrations of mechanical structure efficiently, and systems [71–74].
428 For FOWTs, the aim of using the SC is to damp the platform oscillations and tower loading. The
429 critical advantage of the SC for the FOWT is observed while operating in region 3. Blade pitch
430 mechanism is not required to regulate the platform stability, a significant issue observed in region 3,
431 and SC addresses the platform’s pitching phenomenon. The SC is based on passive, semi-active, and
432 active control approaches [75]. Passive structural control systems use a set of constant parameters
433 to damp the oscillations. Whereas, the semi-active controllers are mainly tunable over a period of
434 time. Contrary to the passive control approach, active structural control differs based on generating
435 the restoring force with dedicated actuators to address the structure loading and oscillation.

436 Passive and active structural control schemes based on two independent Tuned Mass Dampers
437 (TMDs) to deal with the loading and damp the platform oscillation were designed by M. Lackner
438 et al. [30]. These TMDs were placed in the nacelle of a floating barge, operating in region 2 and
439 3. M. Lackner et al. [30] modified the baseline wind turbine [15] by integrating TMD systems

440 and incorporating passive, semi-active active structural control synthesis. Based on input-output
441 data, a high order design model is created using system identification. The control synthesis is
442 achieved based on the loop shaping mechanism. It was observed that both techniques reduced wind
443 turbine loadings when compared with the baseline wind turbine. On the other hand, the complexity
444 and overall cost were increased due to the addition of TMDs. Moreover, active structural control
445 outperformed in reducing the tower's fore-aft fatigue load at the expense of energy consumption,
446 which may be obtained from the high wind while operating in region 3. However, in region 2,
447 active structural control proved costly, and for this purpose, a hybrid mass damper (HMD) was
448 incorporated to work as passive TMD while operating in region 2.

449 Nacelle-based TMD system used Lackner et al. [30] is redesigned by Namik et al. [31] to
450 examine the impact of actuator dynamics on TMDs. Load reduction and power consumption were
451 also investigated for the passive and active control strategies on a barge platform-based FOWT.
452 Although the newly designed controllers followed the simulation trends as shown by Lackner et al.
453 [30] concerning load reduction, the redesigned TMD system achieved platform pitch minimization
454 by consuming relatively less average power.

455 Simplified models of the Mono-pile, Barge, Hywind Spar-buoy, and TLP were used to design an
456 optimal passive TMD based on genetic algorithm by Stewart et al. [32]. This TMD was found to
457 reduce the side-to-side tower fatigue load, which is one of the main components of fatigue loads of
458 FOWTs, better for barge and mono-pile than the TLP and Spar buoy platforms.

459 A Semi-active TMD placed in the nacelle of a wind turbine was used to minimize the incident
460 loads for two platforms: a fixed bottom mono-pile and a TLP, while operating in region 2 and 3
461 [33]. The designed semi-active TMD has a low power energy source, and it swiftly switches between
462 active and passive modes. This mechanism minimizes the side-to-side tower loading of mono-pile
463 and slackline incidents regarding TLP. A platform-based TMD for barge platform FOWT is used
464 to minimize the platform motions and tower loading while operating in region 2, and 3 [76]. A
465 simple static output-feedback mechanism was proposed to generate the stroke, using generalized
466 H_∞ control. Input-output linear model was obtained using system identification. Improved results
467 were obtained in terms of fatigue load and generator power error reduction, while upon comparison,
468 the generalized H_∞ control overperforms H_∞ structural control. Similarly, a Multi-layered Tuned
469 liquid damper (TLD) was developed in [77] for a spar-buoy floating platform and was found useful
470 to minimize platform motions.

471 The traditional passive TMD system's performance was improved by introducing an inerter in
472 the system [78]. The proposed TMD system was placed in the nacelle of the FOWT attached to
473 a barge. The improvement was evaluated in the presence of real incident disturbances, waves and
474 wind. This novel extension of the TMD was found helpful in reducing tower loading. In a relatively
475 similar approach, a STAM (sewing thread artificial muscle) based on thermal actuation attached to
476 mooring lines of the TLP platform was proposed to minimize platform pitching and tower loading
477 for regions 2 and 3 [79]. The active mooring method showed improved results regarding tower
478 loading and pitching motions.

479 **4. Wind and wave forecast algorithms for FOWT control**

480 Incident disturbance forecast is an essential feature of advanced control algorithms like predictive
481 model control and feedforward control. Unlike feedback control, where the controller responds to
482 the disturbance after the system interacts with it, feedforward controllers react to the preview of
483 incoming disturbance ahead of its contact with the system. This approach elevates the performance
484 because the incident disturbance preview provides the controller enough time to respond to the
485 incoming disturbance and adjust parameters to achieve control objectives. Preview-enabled control
486 also enhances the system's structural life as it responds to the incident disturbances ahead of its
487 contact with the system structure.

488 FOWTs are exposed to incident wind and wave disturbance operating in the deep sea. A lot of
489 controllers are designed to stabilize the platform and achieve the control objectives by minimizing
490 the effects of wind and wave disturbances. However, the performance and structural life of FOWTs
491 is still lagging behind when compared with the fixed bottom offshore wind turbines, as most of these
492 control systems are feedback control systems. The incident wind and wave prediction may effectively
493 improve the performance, loading, and structural life of FOWTs with the help of advanced control
494 algorithms like MPC or feedforward control, as proven by the LIDAR based incident wind preview
495 enabled feedforward controllers [29].

496 There are several forecast techniques for wind and wave are reported in the literature, which
497 could be used for preview-based advanced controllers. However, there are issues concerning the
498 prediction horizon length and the forecast quality are to be considered when using these prediction
499 mechanisms. In this section, wind and wave forecast algorithms are discussed.

500 4.1. Wind forecast

501 The wind turbine industry extensively employs the wind forecast to examine a region’s seasonal
502 power production, grid integration, and wind farm design [80]. Based on its application, the length
503 of the prediction horizon of wind forecast ranges from few hours to months, namely; short, medium,
504 and long-term. However, the prediction horizon length for individual wind turbine control systems
505 based on preview information is few seconds. Advanced controllers such as feedforward control
506 require a preview time of a few seconds [51]. Similarly, MPC uses a 5-10s long horizon to compute
507 the input values for system response [52]. Therefore the scope of this paper is limited to the wind
508 forecast for wind turbine control, referred to as ultrashort wind forecast in this paper. An overview
509 of models and devices used for ultra-short wind forecasts is provided below.

510 Statistical time-series models used for wind forecasts are based on the historical site data. Based
511 on the historical wind data, these models tend to learn the underlying patterns in the available
512 data and calculate the future values ahead of time. Widely used conventional statistical models
513 for wind forecast includes autoregressive model (AR) [42, 43], autoregressive moving average model
514 (ARMA) [44], autoregressive integral moving average (ARIMA) [45], fractional-ARIMA [46], and
515 Hammerstein auto-regressive (HAR) [47] etc. Statistical methods heavily rely on historical wind
516 data thus may provide faulty wind forecasts in the absence of enough historical site data.

517 Machine learning (ML) techniques rely on historical data and consider the atmospheric variables
518 that affect the wind speed, such as humidity, elevation, and atmospheric pressure for wind forecast.
519 Therefore, ML methods deal with the nonlinearity of wind better than the statistical methods. ML
520 non-linear prediction methods include artificial neural networks (ANNs) [81, 82], recurrent neural
521 networks (RNN) [83], support vector machine (SVM) [84, 85], least-square support vector machine
522 (LSSVM) [86, 87], Gaussian process (GP) [88], Bayesian networks [89], and extreme learning ma-
523 chine (ELM) [90]. Overfitting and minimum local existence are major drawbacks of ANNs [91].
524 Whereas ELM is proven to have better performance than conventional ANNs and is used for both
525 speed estimation and power forecasting [90, 92, 93]. Hybrid models, a combination of existing
526 model techniques, are also reported in the literature for improved performance. For example, A
527 linear ARIMA and a non-linear ANN are used in a combination for improved wind forecast [94].
528 Similarly, a combination of ELM and ARIMA is shown to have enhanced performance for wind
529 forecast [95].

530 LIDAR is used in the wind turbine industry for several applications such as wind power es-

531 timation and site analysis [96]. They are also used to provide the preview of incident wind for
532 an ultrashort scale horizon upstream of the wind turbine. Wind speed is calculated based on
533 the reflected lasers from the incoming wind particles emitted from LIDAR. Preview measurement
534 of incoming wind speed for FOWT control is discussed in Section 3]. LIDAR-based forecasting
535 techniques are reported to outperform forecasting techniques like ARIMA and persistent methods
536 [97, 98]. However, the higher cost and weather-dependent performance are challenges yet to be
537 further researched.

538 *4.2. Wave forecast*

539 Incident wave accounts for a significant part of FOWT loads when minimizing the platform
540 motions. Therefore, it is also an essential feature to be considered alongside the incident wind in
541 the preview-based FOWT control. Feedforward controllers based on the wind and wave preview may
542 improve the FOWTs loading and platform stability compared to feedback controllers by providing
543 the system enough time to deal with the incoming disturbances. Many wave forecast methods are
544 reported in the literature, such as physics-based models, statistical models, and machine learning
545 models. A discussion on these models is given below.

546 Physics-based models are numerically designed models that solve the complexity of waves based
547 on the physics behind wave mechanics. Physics-based wave forecast models include WAVEWATCH
548 III (WW3) [99], European Center for Medium-range Weather Forecasts (ECMWF) [100], and
549 SWAN (Simulating Waves Nearshore) [101]. These models are generally used for long-term pre-
550 diction horizons over an extensive area. In contrast to the physics-based theory-driven models,
551 data-driven statistical and machine learning provide accurate predictions based on the historical
552 site data. These time-series algorithms extrapolate the past values to provide future wave predic-
553 tions. Statical wave prediction models for wave prediction reported in the literature includes AR,
554 ARMA, ARIMA [48–50]. As compared to statistical models, machine learning prediction models
555 provide improved nonlinear trends identifications in time series wave data. ANN, RNN, CNN, and
556 ANFIS based prediction models [102–106] are some of the examples of machine learning models
557 used for wave prediction in the literature. A comparison of time series-based models and physics-
558 based model (ECMWF) at multiple sites highlights the weakness and strengths of these models
559 [107]. Physics based model performs better for longer prediction horizons, whereas the time series
560 models are better for a shorter prediction horizon. Combinations of physics-based and data-driven

561 statistical models are also reported in the literature [108, 109].

562 **5. Discussion**

563 FOWT technology is still in the pre-commercial phase as compared to the fixed-bottom off-
564 shore wind turbines. The primary concern of FOWT development is the associated cost of energy
565 production and the potential to achieve a cost-effective advantage compared to the fixed-bottom,
566 which is deteriorated by the floating base of FOWT. However, an efficient control mechanism may
567 deal with the shortcoming of the platform, making it economically feasible. These control methods
568 aim to lower LCOE while operating the region below and above the rated wind speed, making it
569 economically feasible. Several control schemes are recently developed for this purpose.

570 *5.1. Comparison between traditional SISO and advanced controllers*

571 The conventional SISO feedback controllers are a natural choice for FOWTs by manipulating
572 the aerodynamic wind load using blade pitch angle and generator torque. Its simple design and
573 easy realization make them a suitable option for fixed-bottom wind turbines. However, the floating
574 platform's natural frequency is lower than the fixed-bottom wind turbines foundation, which causes
575 negative platform damping operating in region III [14]. Controllers designed for fixed-bottom wind
576 turbines may increase the negative platform damping when used for FOWT. Several SISO control
577 strategies are reported in the literature to deal with this issue; refer to Table 1 for details. For
578 example, negative platform damping is addressed by reducing control bandwidth; however, power
579 and speed variations were observed [14]. B. Skaare et al. [17] came up with wind speed estimator-
580 based blade pitch control to deal with the platform's floating motions. Improvement in terms
581 of platform motion damping was achieved at the cost of rotor speed and power output deviation.
582 Jonkman et al. [15] utilized Gain scheduled SISO controller with detuned gains to deal with negative
583 platform damping on a barge platform. However, achieved performance is likely to increase using
584 MIMO controllers, suggested by Jonkman et al. [15]. The coupling between the unmodelled DOF
585 and SISO control loops of FOWT causes inadequate platform motion minimization, power and
586 rotor speed regulation.

587 On the other hand, advanced MIMO controllers can deal with cross-coupling between the un-
588 modeled DOF and control loops better than SISO controllers. These controllers are based on the

589 linearized system model and exhibit superior performance compared with the baseline SISO con-
590 troller. The conflicting blade pitch commands for the platform and rotor regulation are dealt with
591 Individual blade pitch control (IBPC) by creating asymmetric rotor load. However, the platform
592 properties affect the performance of MIMO controllers, as shown in the Table 4. For example, the
593 Barge platform is prone to increased loads due to the inherent platform motion inducing incident
594 waves. MIMO control based on Individual blade pitch control (IBPC) used for barge results in
595 lowered tower loads and platform motion. However, the rotor and power regulation are at a similar
596 level compared to the baseline controller. The reduction in loads is due to increased blade pitch
597 activity. DAC is seen to have no further improvement as it is mainly responsible for lowering the
598 wind disturbances, and the barge platform is mainly affected by incident wave load [22]. Due to its
599 lowered pitch frequency, the Spar-buoy platform is observed to have a slight improvement in the
600 use of IBP based MIMO control compared to other platforms. DAC control effectively reduced the
601 wind disturbance for Spar-buoy, thus leading to better rotor regulation. However, DAC negatively
602 affects the platform motions based on the increased blade pitch activity [21] For the case of TLP,
603 the platform is less affected by the incident waves. IBPC improves the tower loads and platform
604 motions. A significant improvement is observed in the rotor and power regulation which may be
605 attributed to the platform's inherent stability due to tensioned mooring lines. Subsequently, the
606 DAC controller incurs additional improvement by reducing incoming wind disturbance [22].

607 Most of the MIMO controllers for FOWTs are designed around a single operating point. The
608 controller performs well around the operating point; however, moving away from the operating
609 point may lead to performance degradation. To overcome this obstacle, a gain-scheduled controller
610 based on a series of linearized models on a range of operating points improves power regulation
611 and platform motions. LPV controllers offer another switching mechanism to incorporate multiple
612 linear models for a range of operations and deal with the limitation of linearized MIMO models
613 that are only valid around linearization points.

614 Advanced controllers like MPC controllers improve performance while dealing with uncertainties
615 and unmodeled system dynamics. Based on preview wind and wind measurements, MPC corrects
616 the control trajectory based on the plant model at every step. It also allows designers to include
617 the constraints on inputs and states in control design, thus effectively avoiding physical satura-
618 tions. However, MPC is a computationally demanding control mechanism for complex systems like
619 FOWTs. Advanced controllers based on preview information of incident disturbance are superior

620 alternatives to feedback controllers. LIDAR is a valuable addition to improving fixed-bottom wind
 621 turbines; however, LIDAR performance is yet to be evaluated for FOWTs are exposed to wave
 622 disturbances. Details of advanced MIMO controllers is provided in Table 2.

623 Structural controllers based on TMDs adequately reduce the pitching phenomena and reduce
 624 the wind turbine loads, mainly operating in region 3. Controllers we have discussed until now are
 625 mainly based on blade pitch mechanism control. However, structural controllers include additional
 626 DOF that deals with platform motions and tower loading. This way, controller mechanisms ease the
 627 high blade pitch activity and provide a further performance improvement. However, the addition
 628 of TMDs causes an increase in the complexity of the FOWTs. Moreover, the power required to
 629 generate a heavy stroke in active dampers requires further investigation regarding cost-effectiveness
 630 on an industrial scale. List of existing structural controllers is provided in Table 3.

Table 1: Traditional control methods

Method	Model	Platform	Description	Economic viability	OR	
CBP- GSPI [14]	HAWC2/ RIFLEX	SIMO - (Hywind)	Spar-buoy	Region-dependent control based on simple switching process, pitching controller of frequency lower than the platform pitching frequency is employed for region 3.	Improved tower stability. however, degraded power quality and poor rotor speed regulation.	2,3
CBP-GSPI [15, 57]	FAST	Barge, TLP, Spar - buoy	Feedback loop based on Tower-top movement,pitch-to-stall regulation and detuned gains.	Only detuned gains control improves the negative damping issue. Further use of MIMO control is suggested including IBPC.	2,3	
Simple Platform Pitch Control [16]	FAST	Barge	Platform pitch velocity based generator speed control in region 3. Also used IBPC.	Reduced negative damping and blade pitch activity at the cost of the rotor speed fluctuations and power variation. IBPC showed inadequate load reduction.	3	
Control based on estimated wind speed [17]	HAWC2/ RIFLEX	SIMO - (Hywind)	Spar-buoy	Estimator based control mechanism.	Tower Loading, nacelle oscillation and rotor loads are found reduced. However, poor rotor speed regulation and reduced power generated are observed.	3

633 5.2. Impact of the platform on the controllers performance

634 So far, we have discussed a range of controllers designed for FOWTs for their pros and cons.
 635 SISO and advanced MIMO controllers are incorporated to deal with shortcomings associated with
 636 the platform motions. However controller performance may vary based on the type of platform
 637 used for the operation. We have compared several advanced controllers based on the utilized
 638 platform type and their performance in Table 4. Comparison is made in terms of improvement

639 in tower loading, power regulation and platform motions damping to give readers an overview of
640 how control performance may vary based on different platform types. Controllers for the barge
641 platform improved tower loadings and platform motions; however, they perform poorly in terms
642 of power regulations. The TLP platform has inherent stability over its counterpart platforms thus
643 we see improvement compared to the barge platform. MIMO controller based on the IBPC with
644 an extension of DAC ranks higher because it manages to minimize the incident wind disturbance
645 better for the TLP than the barge. Due to lower platform frequency, the spar-buoy platform may
646 not perform well enough, although it has better power regulation, which is mainly due to increased
647 blade pitch activity. However, advanced controllers like MPC and preview-enabled feed-forward
648 controllers exhibit superior performance, especially for the case of power regulations. MPC has a
649 higher ranking also due to the ability to deal with the input and system state constraints.

650 **6. Summary**

651 The control mechanisms we have discussed are all based on model-based design. In complex
652 systems like FOWTs, accurate system modeling is essential for dealing with model uncertainties
653 and complex incident disturbances – wind and wave. In an ideal situation, the plant represents the
654 actual systems and actuators, whereas, in reality, it is a fair approximation of the system. There are
655 expected errors that may result from a poor understanding of the system and un-modeled dynamics,
656 leading to a compromise of system performance. In this case, the model-free control approach may
657 be utilized to represent the plant model and deal with the shortcomings not addressed by first-
658 principle mathematical modeling. Input-output data may be used to deduce a plant representation
659 for the respective controller design after careful assessment and performance evolution. Unlike the
660 model-based design, the data-driven model-free controllers don't rely on the system characteristics,
661 eliminating the need for controller dependency on the plant model. Furthermore, unlike the model-
662 based control approach, in the model-free methodology, the system stability is not relying on the
663 model accuracy [110]. Machine learning techniques may address this issue by finding the optimal
664 control laws by mapping the sensor's output to control actuators. These techniques are based on
665 bio-inspired computational methods, including Genetic Algorithm and Reinforcement and Iterative
666 learning [111]. These algorithms may be used to minimized constraint-based cost functions designed
667 according to the control objectives. One such example of MLC usage for complex structures like
668 FOWTs is reported in the literature [112]. Input-output data is correlated to for a control law

669 $u = k(y)$ and evaluated using a cost function J , as shown in schematic Figure 9. It shows improved
670 performance compared to the baseline controller and demonstrates a viable solution for further
671 research for complex control synthesis for FOWTs.

Table 2: Advanced control methods

Control methods	Model	Platform	Description	Economic viability	OR
MIMO-CBP [20]	FAST	Barge	CBP based Rotor thrust is used to regulate platform pitch and rotor speed.	Poor power and rotor regulation compared with baseline controller. Improved tower loading, platform motions.	3
MIMO-IBPC [20-22]	FAST	Barge, TLP, Spar-Buoy	Asymmetric rotor aerodynamic load is used to regulate the platform pitch and rotor speed.	Tower loads are decreased for the barge, however poor rotor and power regulation. TLP, compared to the Barge and spar-buoy, exhibits less platform movement when IBPC. Due to the lower natural platform frequency, IBPC on Spar-buoy is not useful regardless of the improved rotor regulation.	3
IBPC-DAC [21, 22]	FAST	Barge, TLP, Spar-Buoy	DAC is used as an extension of IBPC with an additional wind disturbance rejection.	DAC has no further improvement on the barge compared to the IBPC applied on a barge. Whereas, when it is utilized on TLP, power and speed regulation are improved with a reduction in side-to-side loads. DAC used on spar-buoy improves rotor speed but increases the blade pitch activity and loads.	3
MIMO (LQR) [23]	DTU-10MW	Spar-Buoy Triple Spar	Effects of the control inputs are analyzed based on how they affects the output for a floating wind turbine in an open loop scenario and an LQR based on observations is synthesized.	Damped various resonances, but observed not being able to suppress the wave excitations entirely.	3
GS-Output feedback H_∞ [18]	FAST	Barge	Generator speed is regulated at the rated value using a gain scheduled controller to keep drive train and tower oscillations low.	Improvements in platform stability and reduced fatigue loads, LPV based GS controller is suggested for further improvements.	3
LPV and LQR based GS [19]	FAST	Barge	GS-LPV and GS-LQR based on output feedback and state feedback are employed.	Improved power regulation and platform pitch minimization is achieved.	3

SMC and IOFL [24]	FAST	Barge	Methods based on LPV control are implemented; to regulate generator speed, and to analyze the effects of incident disturbance on platform motions.	SMC is found to have achieved generator speed regulation better than IOFL for simplified wind turbine models and performance degraded when complex wind turbine models are utilized.	3
NMPC (CBP) [25]	Sandner Model	Spar-buoy	NMPC based on CBP mechanism and generator torque is employed.	Enhanced performance in terms of rotor regulation, platform motion minimization and improved loads. However, the computational cost is significantly higher.	3
N-MPC (IBP) [26]	Sandner Model	Spar-buoy	IBP mechanism is extended based on the collective blade pitch approach.	Lowered pitch and yaw motion, improved speed regulation and reduction of the loads on blades.	3
Linear - MPC (CBP) [27]	Sandner Model	Modified Spar	Linear-MPC based MIMO system is deigned using CBC approach.	Speed and generated power regulation. Improved negative platform pitch motions.	2,3
LIDAR (FF-CBPC) [28]	FAST	TLP	Feed-forward controller based on CBP mechanism is introduced for wind speed regulation.	Improved speed regulation and minimized the loads.	3
LIDAR (FF-CBPC) [29]	FAST	Spar-buoy	CBP FF controller is formulated based on ideal wind speed estimation.	Improved rotor speed and power regulation, along with blades, rotor, and tower load reductions.	3

672 The complex nature of incoming wind and wave limits the control design for FOWTs. Instanta-
673 neous changes in these disturbances, such as wind and wave gusts, may affect the control systems’
674 design for FOWTs. Moreover, if not considered, these flows’ stochastic nature may also degrade the
675 structural life and performance of wind turbines. Incoming disturbances may be modeled to circum-
676 vent these issues. However, it is challenging to design perfect mathematical models of incident wind
677 and wave due to the inherent complicated properties and high dimensions. Data-driven machine
678 learning plays a promising role in solving complex real-life problems. Dynamic Mode Decomposition
679 (DMD) [113], Sparse Identification of Non-linear Dynamics (SINDy) [114], and Koopman Operator
680 Theory [115] are some of the data-driven methods that may be used to understand complex tur-
681 bulent flows and interpret the underlying behaviors. Simplified models of the incident disturbance
682 - wind and wave - may improve the incoming disturbance prediction and estimation process based
683 on these techniques. The LCOE of large FOWT can be reduced by better understanding the effect

684 of incident disturbances on FOWT and subsequent efficient control design.

685 In this review paper, we have reviewed a range of control mechanisms listed in the literature
686 to deal with the shortcomings of FOWT associated with floating platform. SISO and MIMO
687 controllers are discussed based on their improvements in the control objectives of FOWT. structural
688 controllers are analyzed for their unique way of dealing with FOWT loadings. The possibility of
689 utilizing forecasting techniques and model-free control is drawn as well.

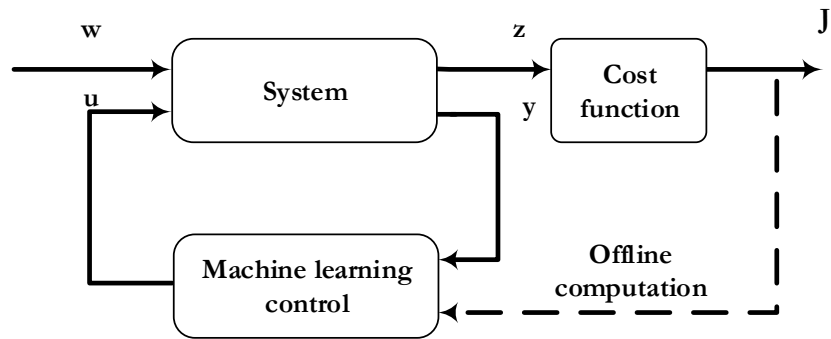


Figure 9: Machine learning control

Table 3: Structural control methods

Control methods	Model	Platform	Description	Economic viability	OR
Active and passive TMD [30]	FAST-SC	Barge/ Fixed bottom monopole	TMD placed in the nacelle, H_{∞} based loop shaping controllers.	Reduced tower loading, Increased complexity and power consumption due to active-TMDs.	2,3
Improved Active and passive TMD [31]	FAST-SC	Barge	Nacelle based redesigned TMDs taking actuator model into consideration.	Fore-aft loads reduction and tower base bending minimization.	2,3
Optimal Passive TMD [32]	FAST-SC	Mono-pile, barge, Hywind spar-buoy and TLP	Optimal passive TMD is developed based on available platforms using genetic algorithm.	Fatigue loads are found reduced for barge and mono-pile better than the TLP and Spar buoy.	2,3
Semi active TMD [33]	FAST-Or-caflex	Mono-pile and TLP (Pelastar)	Nacelle based semi-active TMD.	Minimized side-to-side tower loading of mono-pile and slackline incidents of TLP.	2,3
Active TMD [76]	FAST-SC	Barge	Platform-based TMD, A static output-feedback mechanism is proposed using a generalized H_{∞} control	Fatigue load and generator power error is reduced while reliability and robustness issues of controller designed are found.	2,3
TLD [77]	Numerical methods	Spar-buoy	Nacelle based single and multilayer TLDs are examined and validated.	Enhanced platform pitching motion based on Multilayer TLD than single layer TLD.	-
Passive TMD [78]	FAST-SC	Barge	TMD placed in nacelle, Interter based damping mechanism.	Effectively reduced wind and wave induced loads in comparison with similar traditional TMD control.	2
Active Mooring line control based on STAM [79]	FAST	TLP	STAM-integrated mooring lines.	Platform motions (pitch and roll) and tower bending moment, are minimized.	2,3

The different aspects of FOWTs reviewed for controller design lay a foundation for future work with the following recommendations:

- Most of the research on the control design concerns the wind disturbance and neglects the wave disturbance. It may be advantageous to include the wave information in the control design and the wind disturbance to improve performance further.
- Structural controllers may be further investigated as a viable solution for pitching phenomena and wind turbine loading. Its ability to minimize the platform pitching phenomena without using blade pitch can give designers more freedom to design controllers. However, a cost-effective approach and subsequent validation studies are needed.

Table 4: Performance comparison of MIMO control schemes compared to baseline controller

		Tower Loads	Power regulation	Platform motions	Cost
Barge	IBPC	3	1	3	2
	IBPC- DAC	3	1	3	2
TLP	IBPC	2	3	3	3
	IBPC- DAC	2	4	4	5
Spar-buoy	IBPC	2	3	3	3
	IBPC- DAC	2	4	2	3
	FF-CB	2	5	2	4
	NMPC-CBP	2	5	3	5
	NMPC-IBPC	2	5	3	5

5= Massive improvement
4= Major improvement
3= Minor improvement
2= Slight improvement
1= Decrease in performance

- 700 • The effectiveness of the LIDAR for FOWTs needs to be experimentally validated. Moreover,
701 a device capable of sensing waves similar to LIDAR may help designers include wave preview
702 information alongside wind preview in advanced control mechanisms like MPC.
- 703 • Further development is suggested in the use of prediction algorithms together with advanced
704 controllers. Developing models based on machine learning tools would be of significant ad-
705 vantage, especially in understanding the underlying behaviors and designing optimal control
706 laws.

707 7. Acknowledgment

708 The authors would like to thank Dr. Xiaoni Wu, and Dr. Zeeshan Qaiser for constructive
709 feedback. This work was supported by the National Natural Science Foundation of China [grant
710 no. 51761135012].

711 **Appendix A. Simulation codes and models for FOWTs**

712 The existing system models designed for the fixed-bottom WTs may not be able to reflect the
713 performance of FOWTs. It is mainly due to the moving base of FOWTs and associated motions.
714 Therefore, a system model is required to analyze the FOWTs that incorporates all the significant
715 DOFs, including the floating base. A brief description of some of the major simulation codes used
716 is given below.

717 *Fatigue, Aerodynamics, Structures, and Turbulence (FAST)*

718 The National Renewable Energy Lab (NREL) has designed a modular computer-aided engineer-
719 ing (CAE) open-source software testFatigue, Aerodynamics, Structures, and Turbulence (FAST) to
720 simulate WTs at the desired operating conditions [116]. The FAST code may be used to model WTs
721 by inflow wind, structural dynamics, aerodynamics, and for the case of offshore scenario, mooring
722 line dynamics, hydrodynamics, etc.[117]. FAST uses a Multi-body/modal system (MB/Mod) rep-
723 resentation. The aerodynamics module is based on the Blade element momentum (BEM) theory
724 (quasi-static). At the same time, the hydrodyn modules offer modeling based on Potential flow
725 (PF) and Morison's equation (ME). Furthermore, models based on FAST can generate linearized
726 models useful for the linear control design.

727 A standard multi-megawatt fictitious model of a FOWT is designed based on FAST to assist the
728 development of FOWTs, named NREL 5MW baseline WT [56]. This utility-scale WT is developed
729 based on the publicly available data of existing WTs and simulation models such as WindPACT
730 [118], RECOFF [119], and DOWEC [120].

731 *Horizontal Axis Wind Turbine Code-Second generation (HAWC2)*

732 *Horizontal Axis Wind Turbine Code-Second generation (HAWC2)* is a time-domain commer-
733 cially available code that is mainly used to study the dynamics of fixed bottom WTs operating
734 under external loads [121]. The structural dynamics is based on MBS, whereas the aerodynamic
735 module relies on BEM theory. The WT with a floating base is simulated using the SIMO/RIFLEX
736 code coupled with HAWC2 [55], where SIMO/RIFLEX is used to model the floating foundation
737 and mooring lines, whereas the rotor, blades, and nacelle are designed in HAWC2.

738 A next-generation 10 MW reference WT based on HAWC2 [122] similar to 5 MW baseline WT
739 [56] is also available for the research and development. It was originally designed for the project
740 INNWIND.EU [123].

741 *Bladed*

742 Bladed is a commercial software to simulate WTs for both onshore and offshore sites [124].
743 The FOWTs may be modeled using Bladed by considering the dynamics and the complexity of the
744 system parameters. Bladed code also considers incident wave and wind loads, structural dynamics,
745 aerodynamics, and suitable controller response.

746 The structural dynamics of the Bladed code are based on the multi-body modal (ModMB) sys-
747 tem representation. The aerodynamic module uses both the momentum and blade element model.
748 Simultaneously, an extended version of this model is used to consider models such as Prandtl's tip
749 and root losses, dynamic wake models, and Glauert skew wake model. The hydrodynamic module
750 utilizes the penal method and Morison equation. With a built-in Light detection and ranging (LI-
751 DAR) module, Bladed code may be used to develop advanced control designs based on the LIDAR
752 preview information. The Bladed code can generate the linearized model and state-space matrices,
753 an essential part of linear control theory.

754 As a part of LEANWIND project [125] an 8 MW reference WT [126] is designed based on data
755 available online of WTs and validated using Bladed.

756 *SIMPACK*

757 SIMPACK code is designed to simulate a range of industrial applications such as robotics, auto-
758 motive aerospace, and railway [127]. It is a general-purpose software based on MBS and is applicable
759 for the WTs as well. An extension to the existing code is used for FOWT, connecting HydroDyn
760 and SIMPACK with the help of SIMHydroDyn [128]. These additional modules are to deal with
761 the hydrodynamics and the mooring lines of FOWTs.

762 A comparison of the parameters and properties of the 5 MW, 8 MW and 10 MW reference wind
763 turbines is given in Table Appendix A1.

764

Table Appendix A1: Summary of 5, 8 and 10 MW reference wind turbines

Turbine Name	NREL (5MW)	LEANWIND (8MW)	DTU (10MW)
Number of blades and rotor orientation	3 blades, Upwind	3 blades, Upwind	3 blades, Upwind
765 Rotor Diameter (meters)	126	164	178.3
Tower and Hub height (meters)	90, 87.6	110, 106.3	119, 115.6
Cut in, cut out and rated wind speed (m/s)	3, 25, 11.4	4, 25, 12.5	4, 25, 11.4
Rotor speed range (rpm)	6.9, 12.1	6.3, 10.5	6, 9.6
Hub Nacelle and blade mass (tons)	56.8, 240, 17.7	90, 285, 35	105.5, 446, 41.7

766 *Simplified models*

767 To minimize external disturbances, achieve platform stability, and improved power quality, com-
768 plex simulation codes like FAST are considered an appropriate choice. However, the complex nature
769 of these models may cause problems in the control design process. To circumvent shortcomings as-
770 sociated with the complex models, a simple yet accurate model can be developed to model the
771 essential dynamics and behavior of a FOWT with high accuracy. The effectiveness of simplified
772 models for FOWTs in designing useful controllers has been proven [129]. To facilitate the sim-
773 ple control design process, researchers have produced simplified FOWT models. Below are a few
774 noticeable models available in the literature.

775 *Betti model*

776 To address the complexity of the existing simulation models for the FOWTs, a simplistic control-
777 oriented 2-D rigid model is proposed by Betti et al. [130]. Betti model is designed with 7 states,
778 whereas incident wind and wave disturbances are considered acting in 2-D plane. The schematic
779 of this model is given in Figure Appendix A1. This model may also generate linearized models at
780 various locations within the operating range. Unlike FAST, this model may also be used to calculate
781 the wave disturbance matrix, which provides the incident wave information into the advanced
782 control design process. The Betti model is used for the controller synthesis on a TLP based 5 MW
783 FOWT considering 2-D incident disturbances. However, it was found that the model had a small
784 effect on the platform motions and generated power despite the accurate 2-D motion representation
785 [129, 130].

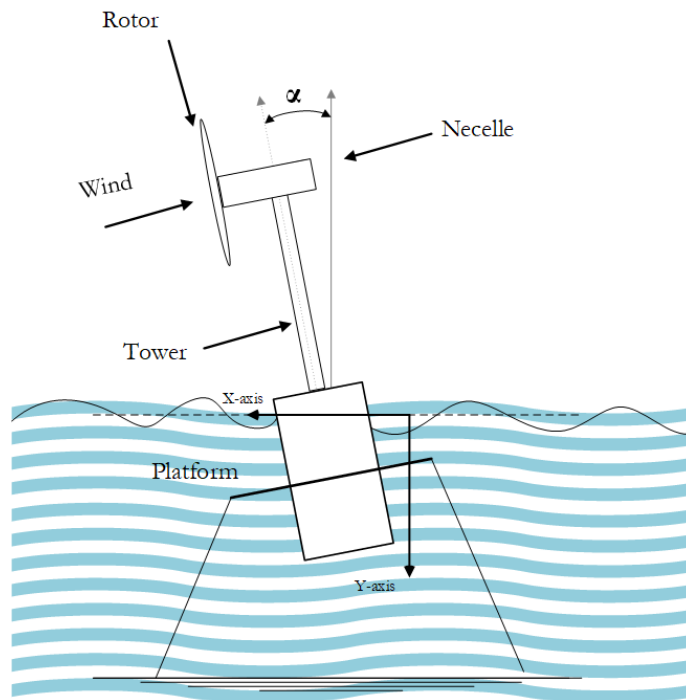


Figure Appendix A1: Adapted layout of Betti model [129]

786 *Sander Model*

787 Sandner et al. [65] designed a less-complex FOWT model for a spar buoy platform as shown
 788 in Figure Appendix A2. The DOFs of this model includes platform motion, rotor speed, nacelle
 789 movement, and pitching angle of the blades. The Sander model has a 2-D structure similar to Betti
 790 model [130] and it's performance is found accurate when compared with the complex FAST model.
 791 However, Sander model may not be used to study FOWT based on other platforms because it is
 792 designed for a spar boy platform, where there is less hydrodynamics involved due to its unique
 793 geometry. Moreover, Sandner model is only used for the 2-D disturbances, and its effectiveness in
 794 a 3-D scenario is yet to be assessed.

795 *Homer model*

796 Homer et al. [131] proposed a simplified and effective control-oriented 3-D design for advanced
 797 control synthesis of a FOWT, as shown in Figure Appendix A3. Like other similar models, the
 798 Homer model also has fewer DOFs (15/16), and it may also be used to generate linearized models

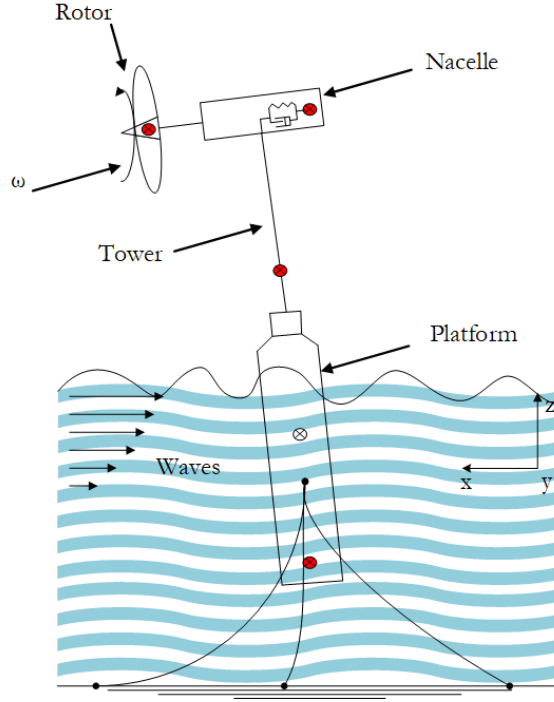


Figure Appendix A2: Adapted layout of Sandner model [65]

799 at a given operating point. The model is capable of reflecting 3-D motion, and assist controller
 800 synthesis to eliminate or reduce the effect of wind and wave disturbances. Furthermore, the Homer
 801 model also comes with an ability to generate wave disturbance matrix. The simplified models are
 802 compared with complex model FAST in terms of their particular characteristics in Table Appendix
 803 A2.

804

Table Appendix A2: Model comparison of existing FOWTs controllers

Model	Nature	DOFs	Incorporates incident wind/wave in controller synthesis
Jonkman [116]	Flexible 3-D	22/24	Wind only
Betti [130]	Rigid 2-D	7	Wind and Wave
Sandner [65]	Flexible 3-D	18	Wind and Wave
Homer [131]	Rigid 3-D	15/16	Wind and Wave

805

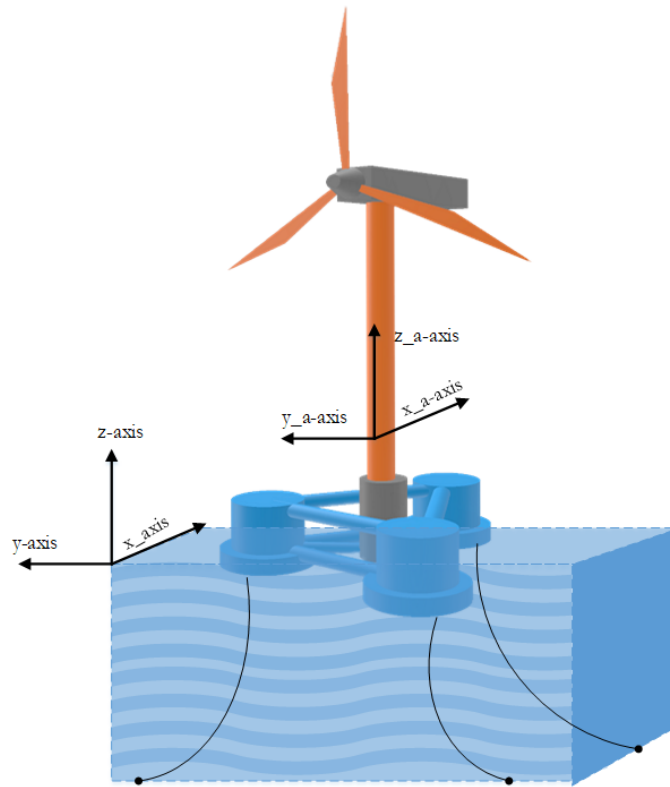


Figure Appendix A3: Adapted layout of Hommer model

806 **References**

- 807 [1] G. W. Statistics, Global wind energy council, Washington, DC, USA.
- 808 [2] U.S. Energy Information Administration, Cost and Performance Characteristics of New Gen-
 809 erating Technologies, Annual Energy Outlook 2019 (2019).
- 810 [3] J. K. Kaldellis, M. Kapsali, Shifting towards offshore wind energy—Recent activity and future
 811 development, Energy Policy 53 (2013) 136–148. doi:<http://dx.doi.org/10.1016/j.enpol.2012.10.032>.
- 812
- 813 [4] J. Wang, S. Qin, S. Jin, J. Wu, Estimation methods review and analysis of offshore extreme
 814 wind speeds and wind energy resources (2015). doi:[10.1016/j.rser.2014.09.042](https://doi.org/10.1016/j.rser.2014.09.042).
- 815 [5] Wind Europe, Floating Offshore Wind Vision Statement, Tech. Rep. June (2017).

- 816 [6] IPCC, Global Warming of 1.5 °C (2018).
817 URL <https://www.ipcc.ch/sr15/>
- 818 [7] K. Borch, N.-E. Clausen, G. Ellis, Environmental and social impacts of wind energy, Tech.
819 rep. (2014).
- 820 [8] K. Dai, A. Bergot, C. Liang, W. N. Xiang, Z. Huang, Environmental issues associated with
821 wind energy - A review, *Renewable Energy* 75 (2015) 911–921. doi:10.1016/j.renene.
822 2014.10.074.
- 823 [9] D. Y. Leung, Y. Yang, Wind energy development and its environmental impact: A review,
824 *Renewable and Sustainable Energy Reviews* 16 (1) (2012) 1031–1039. doi:10.1016/j.rser.
825 2011.09.024.
- 826 [10] J. Lee, F. Zhao, GWEC Global Wind Report, Tech. rep. (2020).
827 URL www.gwec.net
- 828 [11] L. Joyce, Z. Feng, Global Offshore Wind Report 2020, Tech. Rep. August (2020).
829 URL <https://gwec.net/global-offshore-wind-report-2020/www.gwec.net>
- 830 [12] NOAA Ocean Explorer:Types of offshore oil and gas structures.
831 URL [http://appliedmechanicsreviews.asmedigitalcollection.asme.org/article.
832 aspx?doi=10.1115/1.4031175](http://appliedmechanicsreviews.asmedigitalcollection.asme.org/article.aspx?doi=10.1115/1.4031175)
- 833 [13] A. R. Henderson, D. Witcher, Floating offshore wind energy - a review of the current status
834 and an assessment of the prospects, *Wind Engineering* 34 (1) (2010) 1–16. doi:10.1260/
835 0309-524X.34.1.1.
- 836 [14] T. J. Larsen, T. D. Hanson, A method to avoid negative damped low frequent tower vibrations
837 for a floating, pitch controlled wind turbine, *Journal of Physics: Conference Series* 75 (1)
838 (2007) 012073. doi:10.1088/1742-6596/75/1/012073.
- 839 [15] J. M. Jonkman, Dynamics Modeling and Loads Analysis of an Offshore Floating Wind Tur-
840 bine, Ph.D. thesis, National Renewable Energy Laboratory (2007). doi:10.2172/921803.
- 841 [16] M. A. Lackner, Controlling Platform Motions and Reducing Blade Loads for Floating Wind
842 Turbines, *Wind Engineering* 33 (6) (2009) 541–554. doi:10.1260/0309-524X.33.6.541.

- 843 [17] B. Skaare, T. D. Hanson, F. G. Nielsen, Importance of Control Strategies on Fatigue Life of
844 Floating Wind Turbines, in: 26th International Conference on Offshore Mechanics and Arctic
845 Engineering, San Diego, California, 2007, pp. 1–8.
- 846 [18] T. Bakka, H. R. Karimi, N. A. Duffie, Gain Scheduling for Output H_∞ Control of Offshore
847 Wind Turbine, in: Twenty-second (2012) International Offshore and Polar Engineering Con-
848 ference, Rhodes, Greece, 2012, pp. 496–501.
- 849 [19] O. Bagherieh, R. Nagamune, Gain-scheduling control of a floating offshore wind turbine
850 above rated wind speed, *Control Theory and Technology* 13 (2) (2015) 160–172. doi:10.
851 1007/s11768-015-4152-0.
- 852 [20] H. Namik and K. Stol, Individual blade pitch control of floating offshore wind turbines, *Wind*
853 *Energy* 13 (1) (2010) 74–85.
- 854 [21] H. Namik, K. Stol, Individual blade pitch control of a spar-buoy floating wind turbine, *IEEE*
855 *Transactions on Control Systems Technology* 22 (1) (2014) 214–223. doi:10.1109/TCST.
856 2013.2251636.
- 857 [22] H. Namik, K. Stol, Performance analysis of individual blade pitch control of offshore wind
858 turbines on two floating platforms, *Mechatronics* 21 (4) (2011) 691–703. doi:10.1016/j.
859 mechatronics.2010.12.003.
- 860 [23] F. Lemmer, D. Schlipf, P. W. Cheng, Control design methods for floating wind turbines for
861 optimal disturbance rejection, in: *Journal of Physics: Conference Series*, Vol. 753, 2016, p.
862 092006. doi:10.1088/1742-6596/753/9/092006.
- 863 [24] O. Bagherieh, K. Hedrick, R. Horowitz, Nonlinear Control of Floating Offshore Wind Turbines
864 Using Input/Output Feedback Linearization and Sliding Control, in: *Asme Dynamic Systems*
865 *& Control Conference*, 2014, p. 10.
- 866 [25] D. Schlipf, F. Sandner, S. Raach, D. Matha, P. W. Cheng, Nonlinear Model Predictive Control
867 of Floating Wind Turbines, in: the Twenty-third (2013) International Offshore and Polar En-
868 gineering, Anchorage, Alaska, USA, 2013, pp. 440–446. doi:10.1109/ACC.2014.6858718.
- 869 [26] S. Raach, D. Schlipf, F. Sandner, D. Matha, P. W. Cheng, Nonlinear model predictive control
870 of floating wind turbines with individual pitch control, in: *Proceedings of the American*

- 871 Control Conference, Portland, Oregon, USA, 2014, pp. 4434–4439. doi:10.1109/ACC.2014.
872 6858718.
- 873 [27] F. Lemmer, S. Raach, D. Schlipf, P. W. Cheng, Prospects Of Linear Model Predictive Control
874 On A 10MW Floating Wind Turbine, in: the ASME 2015 34th International Conference on
875 Ocean, Offshore and Arctic Engineering, 2015, pp. 1–11. doi:10.1115/OMAE2015-42267.
- 876 [28] S. T. Navalkar, J.-W. van Wingerden, P. A. Fleming, G. A. M. van Kuik, Integrating robust
877 lidar-based feedforward with feedback control to enhance speed regulation of floating wind
878 turbines, in: American Control Conference, IEEE, 2015, pp. 3070–3075.
- 879 [29] D. Schlipf, E. Simley, F. Lemmer, L. Pao, P. W. Cheng, Collective Pitch Feedforward Control
880 of Floating Wind Turbines Using Lidar, in: Twenty-fifth (2015) International Ocean and
881 Polar Engineering Conference, Vol. 2, Kona, Big Island, Hawaii, 2015, pp. 324–331. doi:
882 10.17736/jowe.2015.arr04.
- 883 [30] M. A. Lackner, M. A. Rotea, Structural control of floating wind turbines, *Mechatronics* 21 (4)
884 (2011) 704–719. doi:10.1016/j.mechatronics.2010.11.007.
- 885 [31] H. Namik, M. Rotea, M. Lackner, Active Structural Control with Actuator Dynamics on
886 a Floating Wind Turbine, in: American Institute of Aeronautics and Astronautics, New
887 Horizons Forum and Aerospace Exposition, no. January, 2013, pp. 1–16. doi:10.2514/6.
888 2013-455.
- 889 [32] G. Stewart, M. Lackner, Offshore wind turbine load reduction employing optimal passive
890 tuned mass damping systems, *IEEE Transactions on Control Systems Technology* 21 (4)
891 (2013) 1090–1104. doi:10.1109/TCST.2013.2260825.
- 892 [33] A. R. Tsouroukdissian, S. Park, P. Pourazarm, W. L. Cava, M. Lackner, S. Lee, J. Cross-
893 Whiter, Smart Novel Semi-Active Tuned Mass Damper for Fixed-Bottom and Floating Off-
894 shore Wind, in: Offshore Technology Conference, 2016, pp. 1–17. doi:10.4043/26922-MS.
- 895 [34] Harsh S. Dhiman, *Machine Learning in Wind Forecasting*, 2020.
- 896 [35] S. Karasu, A. Altan, Z. Saraç, R. Hacıoğlu, Prediction of wind speed with non-linear au-
897 toregressive (NAR) neural networks, in: 2017 25th Signal Processing and Communications
898 Applications Conference (SIU), IEEE, 2017, pp. 1–4.

- 899 [36] S. Karasu, A. Altan, Z. Saraç, R. Hacıoğlu, Estimation of fast varied wind speed based on
900 NARX neural network by using curve fitting, *International Journal of Energy Applications
901 and Technologies* 4 (3) (2017) 137–146.
- 902 [37] S. Karasu, A. Altan, Z. Saraç, R. Hacıoğlu, Estimation of wind speed by using regression
903 learners with different filtering methods, in: *1st International Conference on Energy Systems
904 Engineering*, Karabuk, Turkey, 2017.
- 905 [38] L. Li, Z. Yuan, Y. Gao, Maximization of energy absorption for a wave energy converter using
906 the deep machine learning, *Energy* 165 (2018) 340–349.
- 907 [39] L. Li, Z. Yuan, Y. Gao, X. Zhang, Wave force prediction effect on the energy absorption of
908 a wave energy converter with real-time control, *IEEE Transactions on Sustainable Energy*
909 10 (2) (2018) 615–624.
- 910 [40] L. Li, Y. Gao, D. Z. Ning, Z. M. Yuan, Development of a constraint non-causal wave energy
911 control algorithm based on artificial intelligence, *Renewable and Sustainable Energy Reviews*
912 (2020) 110519.
- 913 [41] A. Altan, S. Karasu, E. Zio, A new hybrid model for wind speed forecasting combining long
914 short-term memory neural network, decomposition methods and grey wolf optimizer, *Applied
915 Soft Computing* 100 (2021) 106996.
- 916 [42] U. Schlink, G. Tetzlaff, Wind Speed Forecasting from 1 to 30 Minutes, *Theoretical and Applied
917 Climatology* 60 (1) (1998) 191–198. doi:10.1007/s007040050043.
- 918 [43] T. Gneiting, K. Larson, K. Westrick, M. G. Genton, E. Aldrich, Calibrated Probabilistic Fore-
919 casting at the Stateline Wind Energy Center, *Journal of the American Statistical Association*
920 101 (475) (2006) 968–979. doi:10.1198/016214506000000456.
- 921 [44] J. L. Torres, A. Garcia, M. De Blas, A. De Francisco, Forecast of hourly average wind speed
922 with ARMA models in Navarre (Spain), *Solar Energy* 79 (1) (2005) 65–77.
- 923 [45] A. Sfetsos, A novel approach for the forecasting of mean hourly wind speed time series,
924 *Renewable energy* 27 (2) (2002) 163–174.

- 925 [46] R. G. Kavasseri, K. Seetharaman, Day-ahead wind speed forecasting using f-ARIMA models,
926 *Renewable Energy* 34 (5) (2009) 1388–1393.
- 927 [47] O. Ait Maatallah, A. Achuthan, K. Janoyan, P. Marzocca, Recursive wind speed forecasting
928 based on Hammerstein Auto-Regressive model, *Applied Energy* 145 (2015) 191–197. doi:
929 10.1016/j.apenergy.2015.02.032.
- 930 [48] F. Fusco, J. V. Ringwood, Short-Term Wave Forecasting for Real-Time Control of Wave
931 Energy Converters, *IEEE TRANSACTIONS ON SUSTAINABLE ENERGY* 1 (2) (2010)
932 99–106. doi:10.1109/TSTE.2010.2047414.
- 933 [49] Y. Pena Sanchez, J. Ringwood, A Critical Comparison of AR and ARMA Models for Short-
934 term Wave Forecasting, *Proceedings of the Twelfth European Wave and Tidal Energy Con-*
935 *ference* (2017) 9611—9616.
- 936 [50] M. Ge, E. C. Kerrigan, Short-term ocean wave forecasting using an autoregressive moving
937 average model, in: *2016 UKACC 11th International Conference on Control (CONTROL)*,
938 *IEEE*, 2016, pp. 1–6.
- 939 [51] F. Dunne, L. Y. Pao, D. Schlipf, A. K. Scholbrock, Importance of Lidar Measurement Tim-
940 ing Accuracy for Wind Turbine Control *, *2014 American Control Conference* (2014) 3716–
941 3721doi:10.1109/ACC.2014.6859337.
- 942 [52] D. Schlipf, D. J. Schlipf, M. Kühn, Nonlinear model predictive control of wind turbines using
943 LIDAR, *Wind Energy* 16 (2013) (2013) 1107–1129. doi:10.1002/we.
- 944 [53] A. Betz, Introduction to the theory of flow machines, *Introduction to the Theory of Flow*
945 *Machines* (1966) 5–6.
- 946 [54] A. E. Samani, J. D. de Kooning, N. Kayedpour, N. Singh, L. Vandeveld, The impact of
947 pitch-to-stall and pitch-to-feather control on the structural loads and the pitch mechanism of
948 a wind turbine, *Energies* 13 (17). doi:10.3390/en13174503.
- 949 [55] B. Skaare, T. D. Hanson, F. G. Nielsen, R. Yttervik, A. M. Hansen, Integrated Dynamic Anal-
950 ysis of Floating Offshore Wind Turbines, in: *European Wind Energy Conf. and Exhibition*,
951 *Milan, Italy*, 2007.

- 952 [56] J. Jonkman, S. Butterfield, W. Musial, G. Scott, Definition of a 5-MW Reference Wind
953 Turbine for Offshore System Development, Tech. Rep. February, National Renewable Energy
954 Laboratory (2009).
- 955 [57] D. Matha, Model Development and Load Analysis of an Offshore Wind Turbine, Tech. rep.,
956 University of Colorado - Boulder (2010). doi:10.2172/973961.
- 957 [58] G. Bir, Multi-blade coordinate transformation and its application to wind turbine analysis,
958 in: 46th AIAA aerospace sciences meeting and exhibit, 2008, p. 1300.
- 959 [59] F. Lemmer, S. Raach, D. Schlipf, P. W. Cheng, Parametric Wave Excitation Model for
960 Floating Wind Turbines, in: 13th Deep Sea Offshore Wind R&D Conference, EERA Deep-
961 Wind'2016, 20-22 January 2016, Vol. 94, 2016, pp. 290–305. doi:10.1016/j.egypro.2016.
962 09.186.
- 963 [60] H. Namik, Individual blade pitch control of floating offshore wind turbines, Ph.D. thesis, The
964 University of Auckland (2012).
- 965 [61] D. Schlipf, D. J. Schlipf, M. Kühn, Nonlinear model predictive control of wind turbines
966 using LIDAR, Wind Energy 16 (7) (2013) 1107–1129. arXiv:arXiv:1006.4405v1, doi:
967 10.1002/we.
- 968 [62] S. J. E.A Nederkoorn, K. S. R. R. N. E, Optimised Aerodynamics and Control by Nonlinear
969 Model based Predictive Control, in: European Wind Energy Association Conference, 2013,
970 pp. 1–9.
- 971 [63] A. Körber, R. King, Model predictive control for wind turbines, in: Proc. of European Wind
972 Energy Conference, 2010, pp. 1–7.
- 973 [64] C. P. Schlipf D, Fleming P, Haizmann F, Scholbrock A, Hofsäß M, Wright A, Field Testing
974 of Feedforward Collective Pitch Control on the CART2 Using a Nacelle-Based Lidar Scanner,
975 Journal of Physics: Conference Series 555 (1) (2014) 12090. doi:10.1088/1742-6596/555/
976 1/012090.
- 977 [65] F. Sandner, D. Schlipf, D. Matha, R. Seifried, P. W. Cheng, Reduced Nonlinear Model of a
978 Spar-mounted Floating Wind Turbine, in: Proceedings of the German Wind Energy Confer-
979 ence (DEWEK), Bremen, Germany, 2012, p. 4.

- 980 [66] E. A. Bossanyi, A. Kumar, O. Hugues-Salas, Wind turbine control applications of turbine-
981 mounted LIDAR, *Journal of Physics: Conference Series* 555 (1) (2014) 12011.
- 982 [67] F. Dunne, L. Y.Pao, A. D.Wright, B. Jonkman, N. Kelley, Adding Feedforward Blade Pitch
983 Control to Standard Feedback Controllers for Load Mitigation in Wind Turbines, *Mechatron-*
984 *ics* 21 (4) (2011) 682–690.
- 985 [68] D. Schlipf, S. Schuler, P. Grau, K. Martin, Look-Ahead Cyclic Pitch Control Using LIDAR, in:
986 *The Science of Making Torque from Wind*, Greece, 2010, pp. 1–7. doi:10.18419/opus-4538.
- 987 [69] T. Mikkelsen, Lidar-based Research and Innovation at DTU Wind Energy – A Review, *Jour-*
988 *nal of Physics: Conference Series* 524 (1) (2014) 012007. doi:10.1088/1742-6596/524/1/
989 012007.
- 990 [70] F. Dunne, L. Pao, A. Wright, B. Jonkman, N. Kelley, Combining standard feedback controllers
991 with feedforward blade pitch control for load mitigation in wind turbines, in: *48th AIAA*
992 *Aerospace Sciences Meeting Including the New Horizons Forum and Aerospace Exposition*,
993 Orlando, Florida, 2010, p. 18.
- 994 [71] B. F. Spencer, M. K. Sain, Controlling buildings: a new frontier in feedback, *The Shock and*
995 *vibration digest* 30 (4) (1998) 267–281.
- 996 [72] H. Li, X. Jing, H. R. Karimi, Output-feedback-based H_∞ control for vehicle suspension
997 systems with control delay, *IEEE Transactions on Industrial Electronics* 61 (1) (2014) 436–
998 446.
- 999 [73] W. He, S. Zhang, S. S. Ge, Adaptive control of a flexible crane system with the boundary
1000 output constraint, *IEEE Transactions on Industrial Electronics* 61 (8) (2014) 4126–4133.
- 1001 [74] H. Li, J. Yu, C. Hilton, H. Liu, Adaptive sliding-mode control for nonlinear active suspension
1002 vehicle systems using T–S fuzzy approach, *IEEE Transactions on Industrial Electronics* 60 (8)
1003 (2013) 3328–3338.
- 1004 [75] B. F. Spencer Jr, S. Nagarajaiah, State of the art of structural control, *Journal of structural*
1005 *engineering* 129 (7) (2003) 845–856.

- 1006 [76] X. Li, H. Gao, Load mitigation for a floating wind turbine via generalized H_∞ structural
1007 control, IEEE Transactions on Industrial Electronics 63 (1) (2016) 332–342. doi:10.1109/
1008 TIE.2015.2465894.
- 1009 [77] M. Ha, C. Cheong, Pitch motion mitigation of spar-type floating substructure for offshore
1010 wind turbine using multilayer tuned liquid damper, Ocean Engineering 116 (2016) 157–164.
1011 doi:10.1016/j.oceaneng.2016.02.036.
- 1012 [78] Y. Hu, M. Z. Q. Chen, Passive structural control with inerters for a floating offshore wind
1013 turbine, in: 36th Chinese Control conference, 2017, pp. 9266–9271. doi:10.23919/ChiCC.
1014 2017.8028833.
- 1015 [79] Y. Li, Z. Wu, Stabilization of floating offshore wind turbines by artificial muscle based active
1016 mooring line force control, in: Proceedings of the American Control Conference, 2016, pp.
1017 2277–2282. doi:10.1109/ACC.2016.7525257.
- 1018 [80] H. S. Dhiman, D. Deb, A Review of Wind Speed and Wind Power Forecasting Techniques,
1019 arXivarXiv:2009.02279.
- 1020 [81] Z.-h. Guo, J. Wu, H.-y. Lu, J.-z. Wang, A case study on a hybrid wind speed forecasting
1021 method using BP neural network, Knowledge-based systems 24 (7) (2011) 1048–1056.
- 1022 [82] G. Li, J. Shi, On comparing three artificial neural networks for wind speed forecasting, Applied
1023 Energy 87 (7) (2010) 2313–2320.
- 1024 [83] T. G. Barbounis, J. B. Theocharis, Locally recurrent neural networks for long-term wind
1025 speed and power prediction, Neurocomputing 69 (4-6) (2006) 466–496.
- 1026 [84] M. A. Mohandes, T. O. Halawani, S. Rehman, A. A. Hussain, Support vector machines for
1027 wind speed prediction, Renewable Energy 29 (6) (2004) 939–947.
- 1028 [85] A. Gani, K. Mohammadi, S. Shamshirband, T. A. Altameem, D. Petković, A combined
1029 method to estimate wind speed distribution based on integrating the support vector machine
1030 with firefly algorithm, Environmental Progress & Sustainable Energy 35 (3) (2016) 867–875.
- 1031 [86] J. Zhou, J. Shi, G. Li, Fine tuning support vector machines for short-term wind speed fore-
1032 casting, Energy Conversion and Management 52 (4) (2011) 1990–1998. doi:10.1016/j.
1033 enconman.2010.11.007.

- 1034 [87] D. Petković, S. Shamshirband, N. B. Anuar, H. Saboohi, A. W. A. Wahab, M. Protić, E. Zal-
1035 nezhad, S. M. A. Mirhashemi, An appraisal of wind speed distribution prediction by soft com-
1036 puting methodologies: a comparative study, *Energy conversion and Management* 84 (2014)
1037 133–139.
- 1038 [88] H. Mori, E. Kurata, Application of gaussian process to wind speed forecasting for wind power
1039 generation, in: *2008 IEEE International Conference on Sustainable Energy Technologies,*
1040 *ICSET 2008, IEEE, 2008, pp. 956–959. doi:10.1109/ICSET.2008.4747145.*
- 1041 [89] G. Li, J. Shi, Applications of Bayesian methods in wind energy conversion systems, *Renewable*
1042 *Energy* 43 (2012) 1–8.
- 1043 [90] H. Liu, H.-q. Tian, Y.-f. Li, Four wind speed multi-step forecasting models using extreme
1044 learning machines and signal decomposing algorithms, *Energy conversion and management*
1045 100 (2015) 16–22.
- 1046 [91] Z. Guo, W. Zhao, H. Lu, J. Wang, Multi-step forecasting for wind speed using a modified
1047 EMD-based artificial neural network model, *Renewable Energy* 37 (1) (2012) 241–249.
- 1048 [92] V. Nikolić, S. Motamedi, S. Shamshirband, D. Petković, S. Ch, M. Arif, Extreme learning
1049 machine approach for sensorless wind speed estimation, *Mechatronics* 34 (2016) 78–83.
- 1050 [93] S. Shamshirband, K. Mohammadi, C. W. Tong, D. Petković, E. Porcu, A. Mostafaeipour,
1051 S. Ch, A. Sedaghat, Application of extreme learning machine for estimation of wind speed
1052 distribution, *Climate dynamics* 46 (5-6) (2016) 1893–1907.
- 1053 [94] E. Cadenas, W. Rivera, Wind speed forecasting in three different regions of Mexico, using a
1054 hybrid ARIMA–ANN model, *Renewable Energy* 35 (12) (2010) 2732–2738.
- 1055 [95] J. Wang, J. Hu, K. Ma, Y. Zhang, A self-adaptive hybrid approach for wind speed forecasting,
1056 *Renewable Energy* 78 (2015) 374–385.
- 1057 [96] E. Simley, L. Pao, R. Frehlich, B. Jonkman, N. Kelley, Analysis of wind speed measurements
1058 using continuous wave LIDAR for wind turbine control, in: *49th AIAA Aerospace Sciences*
1059 *Meeting including the New Horizons Forum and Aerospace Exposition, 2011, p. 263.*

- 1060 [97] L. Valdecabres, A. Peña, M. Courtney, L. von Bremen, M. Kühn, Very short-term forecast
1061 of near-coastal flow using scanning lidars, *Wind energy science* 3 (1) (2018) 313–327.
- 1062 [98] E. Simon, M. Courtney, N. Vasiljevic, Minute-scale wind speed forecasting using scanning
1063 lidar inflow measurements, *Wind Energy Science Discussions* (2018) 1–30.
- 1064 [99] WAVEWATCH III (WW3).
1065 URL <https://polar.ncep.noaa.gov/waves/wavewatch/>
- 1066 [100] Forecasts — ECMWF.
1067 URL <https://www.ecmwf.int/en/forecasts>
- 1068 [101] SWAN.
1069 URL [https://www.tudelft.nl/citg/over-faculteit/afdelingen/
1070 hydraulic-engineering/sections/environmental-fluid-mechanics/research/swan](https://www.tudelft.nl/citg/over-faculteit/afdelingen/hydraulic-engineering/sections/environmental-fluid-mechanics/research/swan)
- 1071 [102] M. C. Deo, C. S. Naidu, Real time wave forecasting using neural networks, *Ocean engineering*
1072 26 (3) (1998) 191–203.
- 1073 [103] T. Sadeghifar, M. Nouri Motlagh, M. Torabi Azad, M. Mohammad Mahdizadeh, Coastal
1074 wave height prediction using Recurrent Neural Networks (RNNs) in the south Caspian Sea,
1075 *Marine Geodesy* 40 (6) (2017) 454–465.
- 1076 [104] C. Ni, X. Ma, Y. Bai, Convolutional Neural Network based power generation prediction of
1077 wave energy converter, in: 2018 24th International Conference on Automation and Computing
1078 (ICAC), IEEE, 2018, pp. 1–6.
- 1079 [105] A. Akpınar, M. Özger, M. I. Kömürcü, Prediction of wave parameters by using fuzzy inference
1080 system and the parametric models along the south coasts of the Black Sea, *Journal of Marine
1081 Science and Technology* 19 (1) (2014) 1–14.
- 1082 [106] M. Wu, C. Stefanakos, Z. Gao, S. Haver, Prediction of short-term wind and wave conditions for
1083 marine operations using a multi-step-ahead decomposition-ANFIS model and quantification
1084 of its uncertainty, *Ocean Engineering* 188 (2019) 106300.
- 1085 [107] G. Reikard, P. Pinson, J.-R. Bidlot, Forecasting ocean wave energy: The ECMWF wave
1086 model and time series methods, *Ocean Engineering* 38 (10) (2011) 1089–1099.
1087 URL <http://www.sciencedirect.com/science/article/pii/S0029801811000837>

- 1088 [108] F. Woodcock, C. Engel, Operational consensus forecasts, *Weather and forecasting* 20 (1)
1089 (2005) 101–111.
- 1090 [109] F. Woodcock, D. J. M. Greenslade, Consensus of numerical model forecasts of significant wave
1091 heights, *Weather and Forecasting* 22 (4) (2007) 792–803.
- 1092 [110] Z. S. Hou, Z. Wang, From model-based control to data-driven control: Survey, classification
1093 and perspective, *Information Sciences* 235 (2013) 3–35. doi:10.1016/j.ins.2012.07.014.
1094 URL <http://dx.doi.org/10.1016/j.ins.2012.07.014>
- 1095 [111] S. L. Brunton, B. R. Noack, Closed-Loop Turbulence Control: Progress and Challenges,
1096 *Applied Mechanics Reviews* 67 (5) (2015) 050801. doi:10.1115/1.4031175.
1097 URL [http://appliedmechanicsreviews.asmedigitalcollection.asme.org/article.
1098 aspx?doi=10.1115/1.4031175](http://appliedmechanicsreviews.asmedigitalcollection.asme.org/article.aspx?doi=10.1115/1.4031175)
- 1099 [112] M. B. Kane, Machine Learning Control for Floating Offshore Wind Turbine Individual Blade
1100 Pitch Control, *Proceedings of the American Control Conference 2020-July* (2020) 237–241.
1101 doi:10.23919/ACC45564.2020.9147912.
- 1102 [113] P. J. Schmid, Dynamic mode decomposition of numerical and experimental data, *Journal of*
1103 *fluid mechanics* 656 (2010) 5–28.
- 1104 [114] S. L. Brunton, J. L. Proctor, J. N. Kutz, Discovering governing equations from data by
1105 sparse identification of nonlinear dynamical systems, *Proceedings of the National Academy*
1106 *of Sciences* 113 (15) (2016) 3932–3937.
- 1107 [115] J. L. Proctor, S. L. Brunton, J. N. Kutz, Generalizing Koopman theory to allow for inputs
1108 and control, *SIAM Journal on Applied Dynamical Systems* 17 (1) (2018) 909–930.
- 1109 [116] J. M. Jonkman, M. L. B. Jr, FAST User ’ s Guide, Tech. rep., National Renewable Energy
1110 Laboratory (2005).
- 1111 [117] B. J. Jonkman, J. M. Jonkman, FAST v8.16.00a-bjj User’s Guide, Tech. rep., National Re-
1112 newable Energy Laboratory (2016).
- 1113 [118] D. J. Malcolm, A. C. Hansen, WindPACT turbine rotor design study, National Renewable
1114 Energy Laboratory, Golden, CO 5.

- 1115 [119] Recommendations for design of offshore wind turbines (RECOFF).
1116 URL <https://cordis.europa.eu/project/id/ENK5-CT-2000-00322>
- 1117 [120] F. Goezinne, Terms of reference DOWEC, NEG-Micon. Bunnik.
- 1118 [121] T. J. Larsen, A. M. Hansen, How 2 HAWC2, the user's manual.
- 1119 [122] C. Bak, F. Zahle, R. Bitsche, T. Kim, A. Yde, L. C. Henriksen, M. H. Hansen, J. P. Blasques,
1120 M. Gaunaa, A. Natarajan, The DTU 10-MW reference wind turbine, in: Danish Wind Power
1121 Research, Fredericia, Denmark, 2013.
- 1122 [123] Innwind.eu.
1123 URL <http://www.innwind.eu/>
- 1124 [124] Wind turbine design software — Bladed - DNV GL.
1125 URL <https://www.dnvgl.com/services/wind-turbine-design-software-bladed-3775>
- 1126 [125] LEANWIND.
1127 URL <http://www.leanwind.eu/>
- 1128 [126] C. Desmond, J. Murphy, L. Blonk, W. Haans, Description of an 8 MW reference wind turbine,
1129 in: Journal of Physics: Conference Series, Vol. 753, 2016. doi:10.1088/1742-6596/753/9/
1130 092013.
- 1131 [127] SIMPACK MBS Software — Wind.
1132 URL http://www.simpack.com/industrial_sectors_wind.html
- 1133 [128] D. Matha, F. Beyer, Offshore wind turbine hydrodynamics modelling in SIMPACK, SIM-
1134 PACK news, July.
- 1135 [129] G. Betti, M. Farina, G. A. Guagliardi, A. Marzorati, R. Scattolini, Development of a Control-
1136 Oriented Model of Floating Wind Turbines, IEEE Transactions on Control Systems Technol-
1137 ogy 22 (1) (2014) 69–82. doi:10.1109/TCST.2013.2242073.
- 1138 [130] G. Betti, M. Farina, A. Marzorati, R. Scattolini, G. A. Guagliardi, Modeling and control of a
1139 floating wind turbine with spar buoy platform, in: 2nd IEEE International Energy Conference
1140 and Exhibition, ENERGYCON 2012, 2012, pp. 189–194. doi:10.1109/EnergyCon.2012.
1141 6347749.

1142 [131] J. R. Homer, R. Nagamune, Physics-Based 3-D Control-Oriented Modeling of Floating Wind
1143 Turbines, IEEE Transactions on Control Systems Technology 26 (1) (2018) 14–26. doi:
1144 10.1109/TCST.2017.2654420.